# WAVES IN CYLINDRICAL SHELLS WITH CIRCUMFERENTIAL SUBMEMBERS: A MATRIX APPROACH

# Z. WANG AND A. N. NORRIS

Department of Mechanical and Aerospace Engineering, Rutgers University, Piscataway, New Jersey 08855-0909, U.S.A.

(Received 2 March 1993, and in final form 14 January 1994)

A matrix approach is proposed to investigate waves in circular cylindrical thin shells jointed with circular plates. Both the general propagator matrix and S-matrix formalisms are presented, with emphasis on the latter. The loss of computational accuracy due to the inevitable exponentially growing terms in a propagator matrix is completely avoided by using the S-matrix. This paper demonstrates implementation of S-matrix methods for analyzing waves in complex shell structures with axial symmetry. The basic elements are laid out in detail, including the S-matrix for cylindrical shells, the propagator matrix and the asymptotic S-matrix for plates, and both the propagator matrix and the S-matrix for junctions of cylindrical thin shells with internal and/or external circular plates and for multi-channel elements. The general approach is demonstrated for several examples of cylindrical shells with periodic stiffeners and sub-elements. Dispersion curves are computed and compared with previous results.

#### 1. INTRODUCTION

We are concerned here with wave propagation on circular cylindrical thin shells jointed with circular thin plates for both low and high frequency ranges. The terminologies "high frequencies" and "low frequencies" need to be defined clearly since they are used repeatedly. Let L be a typical propagation distance on the structure, and let K be the largest structural number, at a given frequency. In the high frequency range we have  $KL \gg 1$ , whereas  $KL \leqslant O(1)$  at low frequencies. Classical thin plate and thin shell theories are employed here, which require that  $Kh \ll 1$ , with h the structural thickness. The high frequency range is therefore compatible with the plate and shell theories as long as  $L \gg h$ . Our purpose is to describe the scattering matrix approach, which turns out to be a numerically stable approach at high frequencies. The method will be compared with the better-known propagator matrix approach, which is numerically stable at low frequencies, but fails at high frequencies.

The propagator matrix method is well developed in physics and seismology, with the pioneering work attributed to Thomson [1] and Haskell [2]. It was introduced into the general area of dynamic analysis of continuous elastic systems by Lin and Donaldson [3]. A computational difficulty arises associated with loss of precision because of growing exponential terms in the propagator matrices. This difficulty can be removed by reformulating the matrix (see reference [4]) or considering high order minors of the original matrices (see reference [5]). Unfortunately, as pointed out by Kennett [6], some difficulties still remain, since individual matrix elements are needed for transmission coefficients.

Therefore, Kennett [7, 8] developed a reflection and transmission matrix method in which the matrices contain no growing exponential terms, and so completely avoids loss-of-precision problems. In this paper, we propose a methodology similar to that of Kennett [8] for cylindrical shells and plates, based upon scattering matrices, or S-matrices, a name given by Redheffer [9]. The use of S-matrices is common in quantum mechanical wave descriptions, but is equally valid for classical waves. Growing exponential terms occur in seismological applications only when waves have an incident angle beyond a critical value. In structural acoustics, however, these pernicious terms are always present due to the existence of evanescent flexural waves. This means that if the structure contains many flexural wavelengths the only way to proceed is the S-matrix approach. This is the major motivation of this paper: in short, we contend that the S-matrix is more efficient than the propagator matrix in structural acoustics applications. There are only a few papers applying the S-matrix method to structures; for example, Yong and Lin [10, 11] investigated dynamic response of truss-type structural networks, and von Flotow [12] considered disturbance propagation in assemblages of slender structural members (beams, cables and rods) connected by junctions. As we will see, the S-matrix is intimately related to reflection and transmission matrices for structural elements [13]. No work has been reported using the method for waves propagating on complex structures made of cylindrical shells and circular plates. We note that the state space method used by Tavakoli and Singh [14, 15] is actually the propagator matrix method, as is the method for one-segment shells used by Kalnins [16]. The segmentation method proposed by Kalnins [16] can avoid the loss of accuracy in the process of computing the natural frequencies of mode shapes. However, it results in a system of 2m linear homogeneous matrix equations with 2m unknowns, where m is the number of segments needed to obtain accurate solutions, which increases with frequency.

The main objective in this paper is to introduce the S-matrix approach for structural dynamics, with specific examples of plate—shell structures described. The paper is organized as follows. The general theory is first developed in section 2, where we cast the structural equations as a first order systems of ODEs. The general propagator matrix and S-matrix formalism are introduced in section 2, and rules for using the S-matrix are derived. For example, it is demonstrated how the multi-channel S-matrix can be found from more elementary S-matrices. In sections 3–6 we describe applications of the general theory to practical structures. The specific form of the ODE governing wave motion on circular cylindrical shells is derived and discussed in section 3, and it is shown to be equivalent to the Donnell—Yu equations [17]. The propagator matrix and the S-matrix for cylindrical shells are given in section 3, while the corresponding analysis for circular plates is outlined in section 4. The T-junction of a cylinder and plate is studied in section 5, and the results of sections 3–5 are combined and applied in section 6 to consider cylindrical shells with periodic substructures of varying complexity. The dispersion curves for free waves are computed and compared with previous work.

# 2. THE PROPAGATOR AND THE S-MATRIX

# 2.1. THE PROPAGATOR MATRIX AND THE WAVE PROPAGATOR

We are concerned with unidimensional structural systems with time harmonic dependence (the term  $e^{-i\omega t}$  will be omitted everywhere). The dynamics at any point on the structure may be described by the state vector  $\mathbf{Z}$ , which has 2m components; m generalized velocities and m forces, where the number m depends on the structure and the theory used to analyze the structure. For a rather wide class of elastic structures [14, 16, 18–21], such

as beams, plates and rotationally symmetric shells, the equations of motion may be written in matrix form.

$$d\mathbf{Z}/dX = i\mathbf{N}\mathbf{Z} + \mathbf{F},\tag{1}$$

where N is a  $2m \times 2m$  matrix and F is a 2m-component external force vector. More detailed discussion of this subject will be presented in section 3, where an example of this governing equation will be given.

The homogeneous solution to equation (1) may be written as

$$\mathbf{Z}(X) = \mathbf{P}(X, X_0)\mathbf{Z}(X_0), \tag{2}$$

where

$$\mathbf{P}(X, X_0) = \mathbf{I} + i \int_{x_0}^x dx_1 \mathbf{N}(x_1) - \int_{x_0}^x dx_1 \mathbf{N}(x_1) \int_{x_0}^{x_1} dx_2 \mathbf{N}(x_2) + \cdots$$
 (3)

This series will converge uniformly if all the elements in **N** are bounded [6]. Even so, a simpler way to obtain **P** will be employed later on for uniform layers. We notice that  $d\mathbf{P}(X, X_0)/dX = i\mathbf{N}\mathbf{P}(X, X_0)$ . The matrix  $\mathbf{P}(X, X_0)$  is defined as the propagator or transfer matrix, which maps the state vector at  $X_0$  to that at X. An alternative, but equally valid, point of view is to represent the dynamics in terms of forward and backward propagating structural waves. The 2m-component wave vector  $\mathbf{v}$  may be represented as

$$\mathbf{v} = (\mathbf{u}^f, \mathbf{u}^b)^{\mathrm{T}},$$

and the *m*-component sub-vectors  $\mathbf{u}^f$  and  $\mathbf{u}^b$  denote forward and backward travelling waves, respectively. The wave propagator matrix  $\mathbf{Q}(X, X_0)$  is then defined such that

$$\mathbf{v}(X) = \mathbf{Q}(X, X_0)\mathbf{v}(X_0). \tag{4}$$

The two viewpoints are connected by the relation

$$\mathbf{Z}(X) = \mathbf{E}(X)\mathbf{v}(X),\tag{5}$$

where **E** is a  $2m \times 2m$  matrix of eigenvectors of **N**. Further details of **E** will be discussed later for cylindrical thin shells and circular plates. Comparison of equation (2) with equation (4) implies

$$\mathbf{P}(X, X_0) = \mathbf{E}(X)\mathbf{Q}(X, X_0)\mathbf{E}^{-1}(X_0). \tag{6}$$

We note that the propagator matrix satisfies the group properties

$$P(X_2, X_0) = P(X_2, X_1)P(X_1, X_0), P(X_1, X_0)^{-1} = P(X_0, X), P(X_0, X_0) = I,$$

which are independent of material properties. The wave propagator satisfies the first two of these, but generally,  $\lim_{X\to X_0} \mathbf{Q}(X,X_0) \neq \mathbf{I}$ , unless the material properties and the structure are continuous at  $X_0$ .

The compact form of the unidimensional vector equation of motion, equation (1), simplifies the calculation of many physical quantities. For example, the time average of energy flux in the X-direction over a period is proportional to the products of real parts of the generalized forces and those of the generalized velocities, and may be written succinctly as

$$\langle F \rangle = -\frac{1}{2} \langle \operatorname{Re} (\mathbf{Z}^{\mathsf{T}}) \mathbf{J} \operatorname{Re} (\mathbf{Z}) \rangle = -\frac{1}{2} \mathbf{Z}^{\mathsf{T}} \mathbf{J} \mathbf{Z}^{*},$$
 (7)

where the asterisk denotes the complex conjugate and

$$\mathbf{J} = \begin{bmatrix} \mathbf{0} & \mathbf{I}_{m \times m} \\ \mathbf{I}_{m \times m} & \mathbf{0} \end{bmatrix}.$$

Premultiplying equation (1) with  $\mathbf{F} = 0$  by  $\mathbf{Z}^{*\mathsf{T}}\mathbf{J}$ , and making use of the fact that  $\mathbf{N}$  satisfies the symplectic relation

$$N^{*T}J = JN.$$

we deduce the identity

$$\frac{\mathrm{d}}{\mathrm{d}X} \left( \frac{1}{2} \mathbf{Z}^{\mathsf{T}} \mathbf{J} \mathbf{Z}^{*} \right) = \operatorname{Re} \left\{ \mathbf{Z}^{*\mathsf{T}} \mathbf{J} \mathbf{F} \right\}. \tag{8}$$

This, combined with equation (7), means that the average flux is conserved at any position on the shell at which there is no applied force.

#### 2.2. DEFINITION OF THE S-MATRIX

In this paper we focus on a third approach, involving the concept of input and output wave vectors for a region. Let  $\mathbf{v}^{in}$  and  $\mathbf{v}^{out}$  represent waves coming into and going out of the region, which may be of any length, and is defined by  $X_{(-)} \leq X \leq X_{(+)}$ . The S-matrix transforms input to output wave vectors according to

$$\mathbf{v}^{out} = \mathbf{S}\mathbf{v}^{in}.\tag{9}$$

The elements of S can be derived from the corresponding wave propagator. Let

$$\mathbf{v}^{in} = (\mathbf{u}_{(-)}^f, \mathbf{u}_{(+)}^b)^{\mathrm{T}}, \qquad \mathbf{v}^{out} = (\mathbf{u}_{(+)}^f, \mathbf{u}_{(-)}^b)^{\mathrm{T}},$$
 (10)

and define the partition of a square matrix, A, of size 2m,

$$\mathbf{A} = \begin{bmatrix} \mathbf{A}_1 & \mathbf{A}_2 \\ \mathbf{A}_3 & \mathbf{A}_4 \end{bmatrix},\tag{11}$$

where  $A_i$ , i = 1, 2, 3, 4, are  $m \times m$  matrices. Comparison of equations (4), (9) and (10) leads to

$$\mathbf{S} = \begin{bmatrix} \mathbf{Q}_1 - \mathbf{Q}_2 \mathbf{Q}_4^{-1} \mathbf{Q}_3 & \mathbf{Q}_2 \mathbf{Q}_4^{-1} \\ -\mathbf{Q}_4^{-1} \mathbf{Q}_3 & \mathbf{Q}_4^{-1} \end{bmatrix}. \tag{12}$$

Physical considerations imply, a posteriori, that  $\mathbf{Q}_4$  must be non-singular. We note that  $\mathbf{Q}_4$  might have exponentially grown elements but  $\mathbf{Q}_4^{-1}$  does not. For instance, the flexural wave propagator for a beam always contains terms of the form  $e^{kL}$ , k being the flexural wavenumber and L>0 the propagation length. The propagator matrix does not distinguish between forward and backward waves, including evanescent ones, which lead to the exponentially growing terms, whereas the S-matrix explicitly avoids them. In summary, we emphasize that the S-matrix method is numerically stable.

The submatrices of **S** are actually the transmission matrix **T** and reflection matrix **R** for the structural region under consideration. Partitioning **S** according to equation (11), we find  $S_1 = T_{(-+)}$ ,  $S_2 = R_{(++)}$ ,  $S_3 = R_{(--)}$ , and  $S_4 = T_{(+-)}$ , where the first and second subscripts indicate the points at which waves come in and go out, respectively.

As an example of the difference between the three methods, consider a periodic structure, with fundamental period  $(X_{(-)}, X_{(+)})$ . The propagation constant,  $\mu$ , is defined by [22]

$$\mathbf{v}_{(+)} = \mathbf{e}^{\mu} \mathbf{v}_{(-)}. \tag{13}$$

Either of the end-vectors can be eliminated in favor of the other, and the resulting equation can be written in terms of wave vector or the state vector as

$$(\mathbf{Q} - \mathbf{I} e^{\mu})\mathbf{v}_{(-)} = 0$$
 or  $(\mathbf{P} - \mathbf{I} e^{\mu})\mathbf{Z}_{(-)} = 0$ , (14)

respectively, where  $\mathbf{Q}$  and  $\mathbf{P}$  are both for the unit period. The dispersion relation for the system is  $\det{(\mathbf{Q} - \mathbf{I} \, \mathbf{e}^{\mu})} = 0$ , or  $\det{(\mathbf{P} - \mathbf{I} \, \mathbf{e}^{\mu})} = 0$ , which are clearly equivalent. However, if flexural waves are being considered and the period is many flexural wavelengths, then both  $\mathbf{P}$  and  $\mathbf{Q}$  contain exponentially large terms, leading to inescapable numerical difficulty. This problem is well known; see, e.g., Roy and Plunkett [23]. Alternatively, equation (13) can be rewritten in terms of the incoming and outgoing vectors, and then one or the other eliminated using the S-matrix for the unit period. In this way we find

$$\begin{bmatrix} \mathbf{S}_1 & \mathbf{0} \\ \mathbf{S}_3 & -\mathbf{I} \end{bmatrix} \begin{bmatrix} \mathbf{u}_{(-)}^f \\ \mathbf{u}_{(-)}^b \end{bmatrix} + e^{\mu} \begin{bmatrix} -\mathbf{I} & \mathbf{S}_2 \\ \mathbf{0} & \mathbf{S}_4 \end{bmatrix} \begin{bmatrix} \mathbf{u}_{(-)}^f \\ \mathbf{u}_{(-)}^b \end{bmatrix} = 0, \tag{15}$$

and the dispersion relation becomes

$$\det \begin{bmatrix} \mathbf{S}_1 e^{-\mu} - \mathbf{I} & \mathbf{S}_2 \\ \mathbf{S}_3 & \mathbf{S}_4 e^{\mu} - \mathbf{I} \end{bmatrix} = 0.$$
 (16)

All matrix elements in equations (15) and (16) are now well behaved numerically, leading to a stable scheme at all frequencies.

# 2.3. THE PROPAGATOR AND S-MATRIX FOR A UNIFORM REGION

The elementary solutions of the basic equation (1) have the form  $\mathbf{Z}(X) = \mathrm{e}^{\mathrm{i}K_x X}\mathbf{Z}(0)$  with a uniform layer or region, where  $K_X$  is any one of the 2m eigenvalues of  $\mathbf{N}$ . In order to derive the propagator and the S-matrix, we first note that the eigenvalues occur in pairs,  $\pm K_X$ , and  $K_{Xj}$ ,  $j=1,\ldots,2m$ , are arranged such that the imaginary parts of  $K_{Xj}$ ,  $j=1,\ldots,m$ , are positive or vanish. Then, the eigenvector matrix  $\mathbf{E}$  of equation (5) is constructed in such a way that its columns are eigenvectors which correspond to, from left to right, the eigenvalues in the matrix  $\mathbf{\Lambda}$ , where

$$\Lambda = \text{diag}[K_{X1},...,K_{Xm},-K_{X1},...,-K_{Xm}].$$

It follows from equation (1) with F = 0 that the matrix  $\Lambda$  satisfies the relation

$$NE = E\Lambda. (17)$$

This can be combined with equation (5) to reduce the ODE (1) for the state vector to an ODE for the wave vector,

$$d\mathbf{v}/dX = i\mathbf{\Lambda}\mathbf{v}.\tag{18}$$

We used the fact that  $\mathbf{E}$  is independent of X within a uniform region, and so this differential equation is only piecewise valid in such regions. The wave vector solution is

$$\mathbf{v}(X) = \mathbf{Q}_{(L_{\mathcal{V}})}(X, X_0)\mathbf{v}(X_0), \tag{19}$$

where the wave propagator for a uniform layer of extent  $d = X - X_0$ ,  $X \ge X_0$ , is

$$\mathbf{Q}_{(L_{\nu})}(X, X_0) = \text{diag} \left[ e^{iK_{X1}d}, \dots, e^{iK_{Xm}d}, e^{-iK_{X1}d}, \dots, e^{-iK_{Xm}d} \right]. \tag{20}$$

The sub-matrices of  $\mathbf{Q}$  are, according to equation (11),  $\mathbf{Q}_2 = \mathbf{Q}_3 = 0$ , and  $\mathbf{Q}_4 = \mathbf{Q}_1^{-1}$ , where

$$\mathbf{O}_1(X, X_0) = \text{diag} \left[ e^{iX_{X_1}(X - X_0)}, \dots, e^{iX_{X_m}(X - X_0)} \right]. \tag{21}$$

The S-matrix then follows from equation (12), as

$$S = \operatorname{diag}(S', S'), \tag{22}$$

where  $S' = Q_1$ . There are clearly no growing exponentials in the S-matrix, and so the difficulty of losing accuracy in computation is totally removed. This is the advantage of the S-matrix method over the propagator matrix method, which contains exponentially large terms.

#### 2.4. THE PROPAGATOR AND S-MATRIX FOR AN INTERFACE

By definition, an interface consists of the junction of uniform regions at which the state vector  $\mathbf{Z}$  is continuous. It therefore follows from equation (5) that the wave vector is discontinuous, with values on either side of the interface related by

$$\mathbf{v}_{(+)} = \mathbf{Q}_{(Int)}\mathbf{v}_{(-)},\tag{23}$$

where

$$\mathbf{Q}_{(Int)} = \mathbf{E}_{(+)}^{-1} \mathbf{E}_{(-)}. \tag{24}$$

It is obvious that  $\mathbf{Q}_{(Int)} = \mathbf{I}$  if and only if the material properties and the structure are continuous at the interface. The S-matrix for an interface can now be obtained from equations (12) and (24).

#### 2.5. FORCED VIBRATION RESPONSE

The general solution to equation (1) is

$$\mathbf{Z}(X) = \mathbf{P}(X, X_0)\mathbf{Z}(X_0) + \int_{X_0}^{X} \mathbf{P}(X, \zeta)\mathbf{F}(\zeta) \,\mathrm{d}\zeta, \tag{25}$$

which can be verified by substitution and using the fact that  $d\mathbf{P}(X, X_0)/dX = i\mathbf{N}\mathbf{P}(X, X_0)$ . The associated equation for the wave vector follows from equations (5) and (6) as

$$\mathbf{v}(X) = \mathbf{Q}_{(Ly)}(X, X_0)\mathbf{v}(X_0) + \int_{X_0}^{X} \mathbf{Q}_{(Ly)}(X, \zeta)\mathbf{E}^{-1}\mathbf{F}(\zeta) \,\mathrm{d}\zeta.$$
 (26)

If the loading is of the concentrated type:

$$\mathbf{F}(\zeta) = \mathbf{F}_0 \delta(\zeta - X_0),$$

then we have  $\mathbf{v}_{(+)}(X_0) = \mathbf{v}_{(-)}(X_0) + \mathbf{E}^{-1}\mathbf{F}_0$ , where the subscripts denote the values just to the right and left of the point of application. We may rewrite this in terms of ingoing and outgoing waves as

$$\mathbf{v}^{out}(X_0) = \mathbf{v}^{in}(X_0) + \mathbf{G}_0, \tag{27}$$

where

$$\mathbf{G}_0 = \mathbf{K}\mathbf{E}^{-1}\mathbf{F}_0, \quad \mathbf{K} = \operatorname{diag}(\mathbf{I}, -\mathbf{I}).$$
 (28)

Now consider the source sandwiched between two regions, A and B, to the left and to the right of the loading, respectively. First eliminate the intermediate fields which represent the waves in A, giving

$$\begin{bmatrix} \mathbf{u}_{(+)}^f \\ \mathbf{u}_{(-)}^b \end{bmatrix}_{(\mathcal{A} + \mathit{Src})} = \mathbf{S}^{\mathcal{A}} \begin{bmatrix} \mathbf{u}_{(-)}^f \\ \mathbf{u}_{(+)}^b \end{bmatrix}_{(\mathcal{A} + \mathit{Src})} + \begin{bmatrix} \mathbf{I} & \mathbf{S}_2^{\mathcal{A}} \\ \mathbf{0} & \mathbf{S}_4^{\mathcal{A}} \end{bmatrix} \mathbf{G}_0$$

for region A and the source. Through the same approach, we find

$$\begin{bmatrix} \mathbf{u}_{(+)}^f \\ \mathbf{u}_{(-)}^b \end{bmatrix}_{(A+Src+B)} = \mathbf{S}^{A+B} \begin{bmatrix} \mathbf{u}_{(-)}^f \\ \mathbf{u}_{(+)}^b \end{bmatrix}_{(A+Src+B)} + \mathbf{S}^{Src} \mathbf{G}_0$$
 (29)

for region A, the source and region B combined, where

$$\mathbf{S}^{Src} = \begin{bmatrix} \mathbf{S}_1^B (\mathbf{I} - \mathbf{S}_2^A \mathbf{S}_3^B))^{-1} & \mathbf{S}_1^B (\mathbf{I} - \mathbf{S}_2^A \mathbf{S}_3^B))^{-1} \mathbf{S}_2^A \\ \mathbf{S}_4^A (\mathbf{I} - \mathbf{S}_3^B \mathbf{S}_2^A)^{-1} \mathbf{S}_3^B & \mathbf{S}_4^A (\mathbf{I} - \mathbf{S}_3^B \mathbf{S}_2^A)^{-1} \mathbf{S}_3^B \mathbf{S}_2^A + \mathbf{S}_4^A \end{bmatrix}.$$

The matrix  $S^{Src}$  represents the radiation from the source, and is clearly in the form of an S-matrix Green function.

#### 2.6. THE S-MATRIX ADDITION RULE

We now consider some of the details necessary for computing the S-matrix of complex structures. Let A and B be two adjacent regions on the structure, either of which could be a uniform section, an interface or a composite region. Regardless of the structural geometry, the material properties at the junction of the two regions should be continuous, so that the wave vector is continuous there. Let  $A = \{X | X \in [X_{(-)}, X_{(0)}]\}$  and  $B = \{X | X \in (X_{(0)}, X_{(+)})\}$ ; then, for regions A and B,

$$\begin{bmatrix} \mathbf{u}_{(0)}^f \\ \mathbf{u}_{(-)}^b \end{bmatrix}_{(A)} = \mathbf{S}^A \begin{bmatrix} \mathbf{u}_{(-)}^f \\ \mathbf{u}_{(0)}^b \end{bmatrix}_{(A)}, \qquad \begin{bmatrix} \mathbf{u}_{(+)}^f \\ \mathbf{u}_{(0)}^b \end{bmatrix}_{(B)} = \mathbf{S}^B \begin{bmatrix} \mathbf{u}_{(0)}^f \\ \mathbf{u}_{(+)}^b \end{bmatrix}_{(B)}, \tag{30}$$

respectively, where  $S^A$  and  $S^B$  are the separate S-matrices, and  $\mathbf{u}_{(0)}^f$  and  $\mathbf{u}_{(0)}^b$  are the forward and backward propagating waves at the junction. Eliminating these from equation (30) and partitioning  $S^A$  and  $S^B$  according to equation (11), we deduce the S-matrix for the composite region:

$$\mathbf{S}^{A+B} \equiv \mathbf{S}^{A} \oplus \mathbf{S}^{B} \equiv \begin{bmatrix} \mathbf{S}_{1}^{B} (\mathbf{I} - \mathbf{S}_{2}^{A} \mathbf{S}_{3}^{B})^{-1} \mathbf{S}_{1}^{A} & \mathbf{S}_{2}^{B} + \mathbf{S}_{1}^{B} (\mathbf{I} - \mathbf{S}_{2}^{A} \mathbf{S}_{3}^{B})^{-1} \mathbf{S}_{2}^{A} \mathbf{S}_{4}^{B} \\ \mathbf{S}_{3}^{A} + \mathbf{S}_{4}^{A} (\mathbf{I} - \mathbf{S}_{3}^{B} \mathbf{S}_{2}^{A})^{-1} \mathbf{S}_{3}^{B} \mathbf{S}_{1}^{A} & \mathbf{S}_{4}^{A} (\mathbf{I} - \mathbf{S}_{3}^{B} \mathbf{S}_{2}^{A})^{-1} \mathbf{S}_{4}^{B} \end{bmatrix}.$$
(31)

The addition rule equation (31) is consistent with Kennett and Kerry's [8] procedure for finding the reflection and transmission coefficients for a composite region.

If the structure B has a termination at its right end, then the same type of addition rule can be used to calculate the  $m \times m$  reflection coefficient matrix for waves incident from the left of A. Thus, the reflection matrix for waves incident onto B from the left is, by definition  $S_3^B$ . The desired reflection coefficient matrix for waves incident on A is then just  $(S^{A+B})_3$ . Note that the only part of  $S^B$  used is  $S_3^B$ , i.e., the rest of  $S^B$  is not required. For example, if B represents a constrained end (free, clamped, etc.) then  $S_3^B$  is the only part that is physically meaningful.

# 2.7. THE MULTI-CHANNEL S-MATRIX

Complex structures can also contain multi-channel sections. We next describe the procedure for determining the S-matrix for the typical multi-channel structural section illustrated in Figure 1. We begin with the S-matrix for the one-to-many joint at the left end,

$$\begin{bmatrix} \mathbf{u}_{(1)}^{b} \\ \mathbf{u}_{(2)}^{f} \\ \vdots \\ \mathbf{u}_{(l)}^{f} \end{bmatrix} = \begin{bmatrix} \mathbf{R}_{(11)} & \mathbf{T}_{(12)} & \cdots & \mathbf{T}_{(1l)} \\ \mathbf{T}_{(21)} & \mathbf{R}_{(22)} & \cdots & \mathbf{T}_{(2l)} \\ \vdots & \vdots & \vdots & \vdots \\ \mathbf{T}_{(l1)} & \mathbf{T}_{(l2)} & \cdots & \mathbf{R}_{(ll)} \end{bmatrix} \begin{bmatrix} \mathbf{u}_{(1)}^{f} \\ \mathbf{u}_{(2)}^{b} \\ \vdots \\ \mathbf{u}_{(l)}^{b} \end{bmatrix},$$
(32)

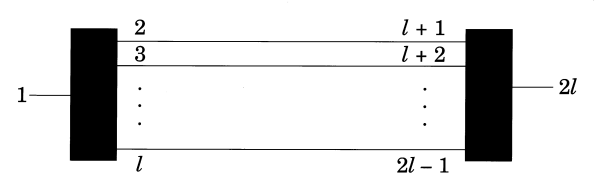


Figure 1. Multi-channels and joints.

where  $\mathbf{T}_{(ij)}$  and  $\mathbf{R}_{(ij)}$ , i, j = 1, 2, ..., l, are transmission and reflection coefficients, respectively. These follow, in general, from the l continuity conditions at the joint. If the channels are in welded contact, and if the thicknesses of those members are small compared to their other dimensions, the conditions are best expressed by first splitting the total state vector into m-component velocity and force sub-vectors,

$$\mathbf{Z} = (\mathbf{Z}^{(v)}, \mathbf{Z}^{(f)})^{\mathrm{T}},\tag{33}$$

for each of the individual state vectors  $\mathbf{Z}_i$ , i = 1,..., l. The continuity conditions then imply the relations

$$\mathbf{Z}_{1}^{(v)} = \mathbf{Z}_{2}^{(v)} = \mathbf{Z}_{3}^{(v)} = \dots = \mathbf{Z}_{l}^{(v)}, \qquad \sum_{i=1}^{l} \mathbf{Z}_{i}^{(f)} = 0,$$
 (34)

expressing the continuity of velocities and the condition that no net force is applied there. It is a routine but unedifying procedure to convert these conditions into the S-matrix of equations (32). The coefficients are given, as an example, in Appendix E for T-junctions of cylindrical shells and interior circular plates. Equation (32) may be written as

$$\begin{bmatrix}
\mathbf{u}_{(2)}^{f} \\
\vdots \\
\mathbf{u}_{(l)}^{f}
\end{bmatrix} = \begin{bmatrix}
\mathbf{S}_{1}^{L} & \mathbf{S}_{2}^{L} \\
\mathbf{S}_{3}^{L} & \mathbf{S}_{4}^{L}
\end{bmatrix} \begin{bmatrix}
\mathbf{u}_{(1)}^{f} \\
\mathbf{u}_{(2)}^{b} \\
\vdots \\
\mathbf{u}_{(l)}^{b}
\end{bmatrix},$$
(35)

where "L" denotes the "left joint", and

$$\mathbf{S}_{1}^{L} = \begin{bmatrix} \mathbf{T}_{(21)} \\ \vdots \\ \mathbf{T}_{(l1)} \end{bmatrix}_{p \times pt}, \qquad \mathbf{S}_{2}^{L} = \begin{bmatrix} \mathbf{R}_{(22)} & \cdots & \mathbf{T}_{(2l)} \\ \vdots & \vdots & \vdots \\ \mathbf{T}_{(l2)} & \cdots & \mathbf{R}_{(ll)} \end{bmatrix}_{p \times p}, \tag{36a}$$

$$\mathbf{S}_{3}^{L} = [\mathbf{R}_{(11)}]_{m \times m}, \qquad \mathbf{S}_{4}^{L} = [\mathbf{T}_{(12)} \quad \cdots \quad \mathbf{T}_{(1l)}]_{m \times p},$$
 (36b)

with p = (l-1)m. It is observed that equation (35) has been written in a form of the single channel matrix, so that its addition rule can be obtained from that for single channels, i.e., equation (31), although it is a multi-channel matrix.

Each separate channel has its own S-matrix,

$$\begin{bmatrix} \mathbf{u}_{(l+1)}^f \\ \mathbf{u}_{(2)}^b \end{bmatrix} = \mathbf{S}^{c2} \begin{bmatrix} \mathbf{u}_{(2)}^f \\ \mathbf{u}_{(l+1)}^b \end{bmatrix}, \quad \cdots \quad \begin{bmatrix} \mathbf{u}_{(2l-1)}^f \\ \mathbf{u}_{(l)}^b \end{bmatrix} = \mathbf{S}^{cl} \begin{bmatrix} \mathbf{u}_{(l)}^f \\ \mathbf{u}_{(2l-1)}^b \end{bmatrix},$$

where  $\mathbf{S}^{ei}$ , i=2,...,l are  $2m \times 2m$  matrices. They can be combined as

$$\begin{bmatrix}
\begin{bmatrix} \mathbf{u}_{(l+1)}^{f} \\ \vdots \\ \mathbf{u}_{(2l-1)}^{f} \end{bmatrix} \\
\begin{bmatrix} \mathbf{u}_{(2)}^{b} \\ \vdots \\ \mathbf{u}_{(l)}^{b} \end{bmatrix}
\end{bmatrix} = \begin{bmatrix} \mathbf{S}_{1}^{C} & \mathbf{S}_{2}^{C} \\ \mathbf{S}_{3}^{C} & \mathbf{S}_{4}^{C} \end{bmatrix} \begin{bmatrix} \mathbf{u}_{(2)}^{f} \\ \vdots \\ \mathbf{u}_{(l)}^{f} \end{bmatrix} ,$$

$$\begin{bmatrix} \mathbf{u}_{(2l-1)}^{b} \\ \vdots \\ \mathbf{u}_{(2l-1)}^{b} \end{bmatrix} ,$$
(37)

with

$$S_i^c = \text{diag}(S_i^{c2}, ..., S_i^{cl}), i = 1, 2, 3, 4,$$

where  $\mathbf{S}_{j}^{ci}$ , i=2,...,l,j=1,...,4, are  $m\times m$  matrices obtained according to equation (11), and  $\mathbf{S}_{i}^{c}$ , i=1,...,4, are  $p\times p$  matrices. The addition rule  $\mathbf{S}^{A+B}=\mathbf{S}^{A}\oplus\mathbf{S}^{B}$  defined in equation (31) can be applied to  $\mathbf{S}^{L}$  and  $\mathbf{S}^{C}$  in equations (35) and (37) even though they have different dimensions. Adding  $\mathbf{S}^{L}$  to  $\mathbf{S}^{C}$  according to the rule gives  $\mathbf{S}^{L+C}=\mathbf{S}^{L}\oplus\mathbf{S}^{C}$ , and we find

$$\begin{bmatrix}
\mathbf{u}_{(l+1)}^{f} \\
\vdots \\
\mathbf{u}_{(2l-1)}^{f}
\end{bmatrix} = \begin{bmatrix}
(\mathbf{S}_{1}^{L+C})_{p \times m} & (\mathbf{S}_{2}^{L+C})_{p \times p} \\
(\mathbf{S}_{3}^{L+C})_{m \times m} & (\mathbf{S}_{4}^{L+C})_{m \times p}
\end{bmatrix} \begin{bmatrix}
\mathbf{u}_{(1)}^{f} \\
\vdots \\
\mathbf{u}_{(2l-1)}^{f}
\end{bmatrix} .$$
(38)

For the right joint, we have

$$\begin{bmatrix} \mathbf{u}_{(2l)}^{\ell} \\ \mathbf{u}_{(l+1)}^{b} \\ \vdots \\ \mathbf{u}_{(2l-1)}^{k} \end{bmatrix} = \begin{bmatrix} \mathbf{S}_{1}^{R} & \mathbf{S}_{2}^{R} \\ \mathbf{S}_{3}^{R} & \mathbf{S}_{4}^{R} \end{bmatrix} \begin{bmatrix} \mathbf{u}_{(l+1)}^{\ell} \\ \vdots \\ \mathbf{u}_{(2l-1)}^{\ell} \end{bmatrix},$$
(39)

where

$$\mathbf{S}_{1}^{R} = [\mathbf{T}_{((2l)(l+1))} \quad \cdots \quad \mathbf{T}_{((2l)(2l-1))}]_{m \times p}, \qquad \mathbf{S}_{2}^{R} = [\mathbf{R}_{((2l)(2l))}]_{m \times m},$$

$$\mathbf{S}_{3}^{R} = \begin{bmatrix} \mathbf{R}_{((l+1)(l+1))} & \cdots & \mathbf{T}_{((l+1)(2l-1))} \\ \vdots & \vdots & \vdots & \vdots \\ \mathbf{T}_{((2l-1)(l+1))} & \cdots & \mathbf{R}_{((2l-1)(2l-1))} \end{bmatrix}_{p \times p}, \qquad \mathbf{S}_{4}^{R} = \begin{bmatrix} \mathbf{T}_{((l+1)(2l))} \\ \vdots \\ \mathbf{T}_{((2l-1)(2l))} \end{bmatrix}_{p \times m}.$$

Combining equations (38) and (39), using equation (31), we finally obtain

$$\begin{bmatrix} \mathbf{u}_{(2l)}^f \\ \mathbf{u}_{(1)}^b \end{bmatrix} = \begin{bmatrix} (\mathbf{S}_1^{L+C+R})_{m \times m} & (\mathbf{S}_2^{L+C+R})_{m \times m} \\ (\mathbf{S}_3^{L+C+R})_{m \times m} & (\mathbf{S}_4^{L+C+R})_{m \times m} \end{bmatrix} \begin{bmatrix} \mathbf{u}_{(1)}^f \\ \mathbf{u}_{(2l)}^b \end{bmatrix}, \tag{40}$$

where  $\mathbf{S}^{L+C+R} = \mathbf{S}^{L+C} \oplus \mathbf{S}^{R}$  is the S-matrix of the multi-channel system.

The addition rule for the multi-channel S-matrix is a "one-shot" approach, in contrast to the step-by-step elimination procedure of reference [11], and it can be easily modified for structures with varieties of geometries. One can also generate rules for combining the propagator matrices for substructures in parallel and in series. In the latter case, the propagators combine by simple multiplication, and the procedure for multi-channel elements is described in Appendix A.

#### 3. WAVES IN CYLINDRICAL THIN SHELLS

Wave propagation in cylindrical shells and circular plates having material and structural inhomogeneities in one co-ordinate direction can be conveniently studied by casting the equations of motion as a first order differential equation for the state vector, in the form of equation (1). Propagator and S-matrix methods appropriate to the 1-D wave equation can then be utilized to full advantage. There is a large volume of literature of related approaches for these particularly structural elements. For example, Kalnins [16] obtained one-dimensional equations for arbitrary rotationally symmetric shells, while Tayakoli and Singh [14] derived a first order ordinary differential equation of an eight-vector from Love's governing equations for circular cylindrical thin shells. Recently, Borgiotti and Rosen [19, 20] presented the equations of motion for circular cylindrical shells in a form of a system of first order differential equations satisfied by a ten-component state vector. Their equation is equivalent to the equations of motion given by Mirsky and Herrmann [24, 25]. An interesting variation on this theme has been presented by Irie et al. [21], who discuss an eight-vector differential equation with respect to the circumferential direction  $\varphi$  for non-circular cylindrical shells. Finally, we note that the long-wavelength behavior of bending waves in periodic thin plates has recently been analyzed by first rewriting the equations of motion as an ordinary differential equation of a four-vector [18].

#### 3.1. EQUATIONS OF MOTION

The equations of motion of an axisymmetric cylindrical thin shell may be written in the form of equation (1), with m = 4. The state vector of the shell is of the form of equation (33), where the sub-vectors of generalized velocities and forces are

$$\mathbf{Z}^{(v)} = \left(\dot{U}, \, \dot{V}, \, -\dot{W}, \, \frac{\partial \, \dot{W}}{\partial X}\right)^{\mathrm{T}}, \qquad \mathbf{Z}^{(f)} = (N_X, \, S_X, \, T_X, \, M_X)^{\mathrm{T}}.$$

The meanings of the components are explained in Appendix B. The state vector and the force vector can be represented as a sum of azimuthal harmonics, each of the form  $\mathbf{Z}_n = \overline{\mathbf{Z}}_n \, \mathrm{e}^{\mathrm{i} n \varphi}$ ,  $\mathbf{f}_n = \overline{\mathbf{f}}_n \, \mathrm{e}^{\mathrm{i} n \varphi}$ . Subscripts n will be suppressed from now on, since only the nth azimuthal harmonic needs to be considered. Starting from the equations of motion, (B9a)–(B9g), we have derived the  $8 \times 8$  matrix  $\mathbf{N}$  and the  $8 \times 1$  vector  $\mathbf{F}$ , with the details given in Appendix C. We notice that  $\mathbf{N}$  may be partitioned as

$$\mathbf{N}(X) = \mathbf{G} \begin{bmatrix} \mathbf{N}_{Mem} & \mathbf{C} \\ \mathbf{J}_4 \mathbf{C}^{*T} \mathbf{J}_4 & \mathbf{N}_{Flex} \end{bmatrix} \mathbf{G}^{-1}, \tag{41}$$

where, and in the rest of this paper, G represents a "transformation matrix" which transforms a vector into a different form. The dimensions and elements of G will be specified each time it is used. See Appendix C for details and definitions of the submatrices and G for equation (41). We note that equation (1) allows for arbitrary X-dependence in the shell parameters, and this is reflected in the possibility that N is a function of X.

The equations of motion for a flat plate can be obtained in the same form as equation (1) by simply allowing the radius R to tend to infinity, with  $N \rightarrow N^{plate}$ , where

$$\mathbf{N}^{plate} = \mathbf{G} \begin{bmatrix} \mathbf{N}_{Mem} & \mathbf{0} \\ \mathbf{0} & \mathbf{N}_{Flex}' \end{bmatrix} \mathbf{G}^{-1}.$$
 (42)

**G** is as before, while  $N_{Mem}$  and  $N'_{Flex}$  follow from equation (41) and Appendix C with  $n/R \rightarrow K_Y$ , which is independent of R. The decoupling between flexural and membrane waves is apparent in equation (42). The shell can also be treated as a flat plate at very high frequencies. To see this, we recall that for acoustic waves  $n \propto \omega$  and for flexural waves

 $n \propto \omega^{1/2}$ . Examining each row of equation (C10) in the limit as  $\omega \to \infty$  leads to the high frequency approximation of **N**, which is the same as  $\mathbf{N}^{plate}$ . Therefore, the flat plate approximation is acceptable when the wavelength is much smaller than the radius of the shell.

The equations of motion presented here explicitly ignore effects due to shear and rotational inertia. The resulting equations and matrices are simpler on this account, but we note that the more sophisticated shell theories which incorporate shear effects have been considered by Tavakoli and Singh [14] and Borgiotti and Rosen [19, 20], among others. The shell theories considered here still reveal the basic features of waves in thin shells. Moreover, it is advantagenous to combine the present thin shell theory with classical thin plate theory to study wave propagation at T-junctions of shells and plates, since the continuity conditions are simple. If the shear effects are included, then at a T-junction the rotation angle of the shell has to match a combination of two quantities: the bending angle and the shearing angle of the plate, making the continuity conditions more complex. In contrast, corresponding quantities match each other in the classical theory.

#### 3.2. EIGENVALUES AND EIGENVECTORS

In order to obtain the propagator matrix and the wave propagator for a uniform layer, we first need to find the eigenvalues and the eigenvectors of **N**. It is generally possible to obtain the linearly independent eigenvectors for **N** even with repeated eigenvalues, as pointed out by Yong and Lin [26]. To simplify the problem further, we reduce the  $8 \times 8$  matrix **N** to a  $4 \times 4$  matrix by first defining an eight-vector  $(\mathbf{Z}_1, \mathbf{Z}_2)^T = \mathbf{G}\mathbf{Z}$ , where  $\mathbf{Z}_1$  and  $\mathbf{Z}_2$  are two four-vectors and **G** is a  $8 \times 8$  matrix with non-zero elements  $g_{11} = g_{34} = g_{52} = g_{73} = 1$ ,  $g_{26} = g_{47} = g_{65} = g_{88} = -1$ . Rewriting equation (1) with  $\mathbf{F} = 0$  as

$$d\mathbf{Z}_1/dX = i\mathbf{N}_1\mathbf{Z}_2, \qquad d\mathbf{Z}_2/dX = i\mathbf{N}_2\mathbf{Z}_1, \tag{43}$$

and substituting  $\mathbf{Z}_1 = e^{iK_XX}\mathbf{Z}_{10}$  and  $\mathbf{Z}_2 = e^{iK_XX}\mathbf{Z}_{20}$ , we obtain

$$(K_X^2 \mathbf{I} - \mathbf{N}_1 \mathbf{N}_2) \mathbf{Z}_{10} = \mathbf{0}. \tag{44}$$

The 4 × 4 matrices  $N_1$ ,  $N_2$  and  $N_1N_2$  are listed in Appendix C. The dispersion relation follows from equation (44), and once  $K_X$  and  $\mathbf{Z}_{10}$  are obtained,  $\mathbf{Z}_{20}$  can be calculated using equation (43).

For each eigenvalue  $K_{Xi}$ , let  $\mathbf{e}_i = \mathbf{G}^{-1}(\mathbf{Z}_{10}, \mathbf{Z}_{20})^{\mathrm{T}}$ , i = 1, ..., 8; then it may be shown that

$$(K_{XI}^* - K_{Xm})\mathbf{e}_I^{*\mathsf{T}}\mathbf{J}\mathbf{e}_m = 0. \tag{45}$$

Hence eigenvectors corresponding to different eigenvalues are orthogonal in the sense of equation (45). However, if  $K_{XI}^* = K_{Xm}$ , then  $\mathbf{e}_I$  and  $\mathbf{e}_m$  do not have to be mutually orthogonal; while if  $K_{XI}$  is not purely real, we always have

$$\mathbf{e}_{l}^{*T}\mathbf{J}\mathbf{e}_{l}=0$$

which means that the evanescent waves give no contribution to the averaged energy flux even if the axial wave vector has a real part.

The dispersion relation for uniform cylindrical shells follows from equation (44) as  $\det (K_x^2 \mathbf{I} - \mathbf{N}_1 \mathbf{N}_2) = 0$ . Let  $k = \sqrt{K_x^2 R^2 + n^2}$ , and define  $\theta$  such that  $K_x R = k \cos \theta$ ,

 $n = k \sin \theta$ ; then the dispersion relation becomes

$$\beta^{2} \left( \frac{1-\nu}{2} \right) k^{8} - \beta^{2} \Omega^{2} \left( \frac{3-\nu}{2} \right) k^{6} + \left[ \beta^{2} \Omega^{4} - \Omega^{2} \left( \frac{1-\nu}{2} \right) + \left( \frac{1-\nu}{2} \right) (1-\nu^{2}) \cos^{4} \theta \right] k^{4}$$

$$+ \left[ \Omega^4 \left( \frac{3-\nu}{2} \right) - \Omega^2 \left( \frac{1-\nu}{2} \right) ((2\nu + 3)\cos^2\theta + \sin^2\theta) \right] k^2 + \Omega^4 - \Omega^6 = 0, \quad (46)$$

where  $\beta^2 = h^2/12R^2$ ,  $\Omega = \omega/\omega_r$  and  $\omega_r = R^{-1}\sqrt{E/\rho(1-v^2)}$  is the ring frequency. We remark that equation (46) is consistent with equation (8) of Pierce [27].

# 4. WAVES IN CIRCULAR THIN PLATES

The equations of motion for the plate are derived from those for the shell by letting  $R \to \infty$ , as discussed above, although they can also be found in textbooks; see, e.g., Love [28]. These equations govern both flexural, or anti-plane, and membrane, or in-plane, motions of the plates. The membrane waves (longitudinal and shear) may be ignored when their wavelengths are much greater than the diameter of the plate. However, the membrane waves must be considered when the wavelengths and the diameter are comparable. This is the case in this paper, since we are concerned with high frequencies. The other reason to consider both flexural waves and membrane waves in the plates is that both wave types are coupled through the connections with waves in the cylinder. In general, it is not possible to obtain a wave eigenvector relation such as equation (17) for the circular plate at all frequencies, because N is not constant as a function of the radial co-ordinate r. One could introduce the idea of differential S-matrices to rectify this, but we prefer to focus on the high frequency limit in which the r-dependence is small. In this section we derive the S-matrix for circular plates at high frequencies; in other words, an asymptotic S-matrix. At lower frequencies, propagator matrix methods can be safely used. The asymptotic S-matrix for the circular plate is one of the main points of this paper.

#### 4.1. EQUATIONS OF MOTION AND SOLUTIONS

The equations of motion for thin plates may be obtained from those for cylindrical thin shells by letting  $R \rightarrow \infty$ . Recalling equation (41), we have

$$\frac{\partial^2 u}{\partial x_1^2} + \frac{1 - \tilde{v}}{2} \frac{\partial^2 u}{\partial x_2^2} + \frac{1 + \tilde{v}}{2} \frac{\partial^2 v}{\partial x_1 \partial x_2} = \frac{\tilde{\rho}(1 - \tilde{v}^2)}{\tilde{E}} \frac{\partial^2 u}{\partial t^2},\tag{47a}$$

$$\frac{1+\tilde{v}}{2}\frac{\partial^2 u}{\partial x_1 \partial x_2} + \frac{1-\tilde{v}}{2}\frac{\partial^2 v}{\partial x_1^2} + \frac{\partial^2 v}{\partial x_2^2} = \frac{\tilde{\rho}(1-\tilde{v}^2)}{\tilde{E}}\frac{\partial^2 v}{\partial t^2},\tag{47b}$$

$$\tilde{D}V^4w + \tilde{\rho}\tilde{h}\frac{\partial^2 w}{\partial t^2} = 0, \tag{47c}$$

where u, v and w are displacements in the  $x_1$ -, and  $x_2$ - and the  $x_3$ -directions, respectively. The displacement components are denoted by lower case letters and the plate parameters have tildes ( $\tilde{}$ ) to distinguish them from the corresponding cylinder quantities. These are the classical equations of motion for thin plates [28]. Plane polar co-ordinates r,  $\varphi$ ,  $x_3$ , with the origin at the center of the plate, will be used from now on. The general solution to

equations (47a)-(47c) is

$$u_{r} = \left[ a \sum_{l=1}^{2} A_{m}^{(l)} \mathbf{H}_{n}^{(l)'}(ar) + \frac{n}{r} \sum_{l=1}^{2} B_{m}^{(l)} \mathbf{H}_{n}^{(l)}(br) \right] e^{in\varphi}, \tag{48a}$$

$$u_{\varphi} = i \left[ \frac{n}{r} \sum_{l=1}^{2} A_{m}^{(l)} H_{n}^{(l)}(ar) + b \sum_{l=1}^{2} B_{m}^{(l)} H_{n}^{(l)'}(br) \right] e^{in\varphi}, \tag{48b}$$

$$w = \sum_{l=1}^{2} \left[ A_f^{(l)} \mathbf{H}_n^{(l)}(cr) + B_f^{(l)} \mathbf{H}_n^{(l)}(icr) \right] e^{in\varphi}, \tag{48c}$$

where  $A_m^{(l)}$ ,  $B_m^{(l)}$ ,  $A_f^{(l)}$ ,  $B_f^{(l)}$ , l=1,2, are constants, and  $H_n^{(l)}$  are Hankel functions. The subscripts f and m indicate flexural and membrane contributions, respectively, and the wavenumbers a, b and c are defined in Appendix D. We note that the general solution for solid circular plates must be finite at the center r=0, implying that  $A_{\alpha}^{(1)}=A_{\alpha}^{(2)}$ , and  $B_{\alpha}^{(1)}=B_{\alpha}^{(2)}$ , for  $\alpha=f$  and m.

#### 4.2. THE PROPAGATOR MATRIX

The state vector for the plate is defined as  $\mathbf{z} = (\mathbf{z}^{(v)}, \mathbf{z}^{(f)})^T$ , to distinguish it from  $\mathbf{Z}$  for the cylinder, and the velocity and force sub-vectors are, by analogy with those for the cylinder,

$$\mathbf{z}^{(v)} = \left(\dot{w}, \dot{u}_{\varphi}, -\dot{u}_{r}, -\frac{\mathrm{d}\dot{w}}{\mathrm{d}r}\right)^{\mathrm{T}}, \qquad \mathbf{z}^{(f)} = (t_{r}, n_{r\varphi}, -n_{r}, m_{r})^{\mathrm{T}}$$
(49)

The state vector is propagated across the plate according to

$$\mathbf{z}(R) = \tilde{\mathbf{P}}\mathbf{z}(r),\tag{50}$$

where the propagator matrix follows from equation (D15) as

$$\tilde{\mathbf{P}} = \mathbf{G} \begin{bmatrix} \mathbf{P}_f(R, r) & \mathbf{0} \\ \mathbf{0} & \mathbf{P}_m(R, r) \end{bmatrix} \mathbf{G}^{-1}.$$
 (51)

The matrices  $\mathbf{P}_f(R, r)$  and  $\mathbf{P}_m(R, r)$  are given in Appendix D, and all elements of  $\mathbf{G}$  vanish except  $g_{11} = g_{26} = g_{54} = g_{67} = g_{83} = 1$ ,  $g_{35} = g_{42} = g_{78} = -1$ . As might be expected for this degenerate structure, the state vector can be split into flexural and membrane constituents: thus  $(\mathbf{z}^{(v)}, \mathbf{z}^{(f)})^{\mathrm{T}} = \mathbf{G}(\mathbf{z}_f, \mathbf{z}_m)^{\mathrm{T}}$ .

# 4.3. THE ASYMPTOTIC S-MATRIX FOR CIRCULAR PLATES

It can be seen from the asymptotic expression equation (D20) for the Hankel function in Appendix D that the propagator matrix contains exponentially growing terms associated with evanescent flexural waves. These cause computational difficulties when frequencies are high, in which case the asymptotic S-matrix is preferable. Combining the results for flexural and membrane waves, equations (D22)–(D24), we find that

$$\mathbf{z} = \widetilde{\mathbf{E}} \begin{bmatrix} \widetilde{\mathbf{u}}^{o} \\ \widetilde{\mathbf{u}}^{i} \end{bmatrix}, \qquad \begin{bmatrix} \widetilde{\mathbf{u}}^{o}(R) \\ \widetilde{\mathbf{u}}^{i}(r) \end{bmatrix} = \widetilde{\mathbf{S}} \begin{bmatrix} \widetilde{\mathbf{u}}^{o}(r) \\ \widetilde{\mathbf{u}}^{i}(R) \end{bmatrix}, \tag{52}$$

where the superscript o and i indicate outgoing and ingoing, relative to the center of the plates, and

$$\mathbf{\tilde{S}} = \operatorname{diag}(\mathbf{\tilde{S}}', \mathbf{\tilde{S}}'), \qquad \mathbf{\tilde{S}}' = \operatorname{diag}(e^{ic\tilde{d}}, e^{-c\tilde{d}}, e^{ia\tilde{d}}, e^{ib\tilde{d}}), 
\mathbf{\tilde{u}}^o = \begin{bmatrix} \mathbf{u}_f^o \\ \mathbf{u}_m^o \end{bmatrix}, \qquad \mathbf{\tilde{u}}^i = \begin{bmatrix} \mathbf{u}_f^i \\ \mathbf{u}_m^i \end{bmatrix}, \qquad \mathbf{\tilde{E}} = \mathbf{G} \begin{bmatrix} \mathbf{E}_f & \mathbf{0} \\ \mathbf{0} & \mathbf{E}_m \end{bmatrix} \mathbf{G}'.$$
(53)

Here, **G** is as in equation (51), and all elements of **G**' vanish except  $g'_{11} = g'_{22} = g'_{33} = g'_{64} = g'_{35} = g'_{46} = g'_{77} = g'_{88} = 1$ . The remaining quantities in these equations are defined in Appendix D. The **S**-matrix relation equation (52) implicitly associates the radially outgoing waves with the "forward" waves. Sometimes it is useful to treat these as the "backward" waves instead, in which case equations (52) becomes

$$\mathbf{z} = \widetilde{\mathbf{E}}' \begin{bmatrix} \widetilde{\mathbf{u}}^i \\ \widetilde{\mathbf{u}}^o \end{bmatrix}, \qquad \begin{bmatrix} \widetilde{\mathbf{u}}^i(r) \\ \widetilde{\mathbf{u}}^o(R) \end{bmatrix} = \widetilde{\mathbf{S}} \begin{bmatrix} \widetilde{\mathbf{u}}^i(R) \\ \widetilde{\mathbf{u}}^o(r) \end{bmatrix}, \tag{54}$$

where, partitioning according to equation (11),  $\tilde{\mathbf{E}}_1' = \tilde{\mathbf{E}}_2$ ,  $\tilde{\mathbf{E}}_2' = \tilde{\mathbf{E}}_1$ ,  $\tilde{\mathbf{E}}_3' = \tilde{\mathbf{E}}_4$  and  $\tilde{\mathbf{E}}_4' = \tilde{\mathbf{E}}_3$ . Both formulations (equations (52) and (54)) are necessary for the examples discussed in section 6.

#### 5. THE T-JUNCTION

Wave propagation across joints of plates has been studied by many authors, including Cremer *et al.* [29], Veshev [30], Romanov [31], Budrin and Nikiforov [32] and Lu *et al.* [33]. Roy and Plunkett [23] considered the coupled bending and longitudinal waves in periodically T-jointed beams using the propagator matrix method. Several methods have been developed for and applied to jointed plates and shells. Some of the approaches and authors include: the classical method of matching the boundary conditions by Smith and Haft [34, 35]; minimization of a Lagrangian, by Harino [36, 37]; the transfer matrix method, by Irie *et al.* [21, 38] and Kobayashi and Irie [39]; the state space method, by Tavakoli and Singh [14, 15] which is equivalent to the propagator matrix method described here; the variational approach, by Cheng and Nicolas [40]; and, finally, the receptance method by Faulkner [41] and Huang and Soedel [42]. More detailed reviews can be found in the papers of Tavakoli and Singh [15] and Huang and Soedel [42]. To the author's knowledge, no investigation has been made of plate—shell structures through the S-matrix approach.

# 5.1. THE CONTINUITY CONDITIONS

The intersection of a cylindrical shell and a circular plate is considered as a ring with infinitesimal cross-section. Hence, the forces and the moments exerted on the shell by the plate are of concentrated type and those exerted on the plate by the shell may be treated as boundary conditions. Based upon these considerations, the continuity conditions at a T-junction can be written as

$$\mathbf{Z}^{(f)}(X_2) - \mathbf{Z}^{(f)}(X_1) \pm \mathbf{z}^{(f)}(X_3) = \mathbf{0}, \qquad \mathbf{Z}^{(v)}(X_2) = \mathbf{Z}^{(v)}(X_1) = \mathbf{z}^{(v)}(X_3)$$
 (55)

(see Figure 2), where the sign in front of  $\mathbf{z}^{(f)}$  should be "+" when the plate is outside the shell and "-" when the plate is inside.

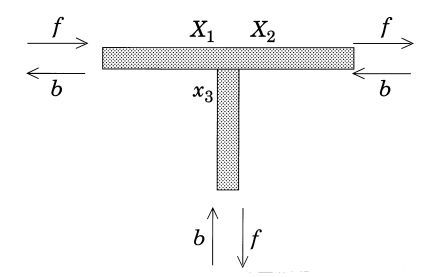


Figure 2. The T-junction.

#### 5.2. T-JUNCTION OF A CYLINDER AND AN INTERNAL ANNULAR CIRCULAR PLATE

As mentioned above, there are many different approaches to investigating waves through joints between members. We focus here on the impedance matrix method and the multi-channel S-matrix method, and both techniques will be described and compared. In general, the impedance approach is preferable at low frequencies, whereas the S-matrix is more natural at higher frequencies for reasons given earlier. The impedance matrix  $\tilde{\mathbf{Y}}$  is defined by

$$\mathbf{z}^{(f)}(R) = \tilde{\mathbf{Y}}(R)\mathbf{z}^{(v)}(R), \tag{56}$$

and can be defined from the boundary conditions at the inner radius r,

$$\tilde{\mathbf{Y}}(R) = [\tilde{\mathbf{P}}_3 + \tilde{\mathbf{P}}_4 \tilde{\mathbf{Y}}(r)][\tilde{\mathbf{P}}_1 + \tilde{\mathbf{P}}_2 \tilde{\mathbf{Y}}(r)]^{-1},$$

where  $\tilde{\mathbf{P}}_i$ , i = 1, 2, 3, 4, are obtained according to equation (11). For example, if r is a free edge, it can be shown by letting  $\tilde{\mathbf{Y}}(r) = 0$  that  $\tilde{\mathbf{Y}}(R) = \tilde{\mathbf{P}}_3 \tilde{\mathbf{P}}_1^{-1}$ , whereas if r is a fixed edge,  $\tilde{\mathbf{Y}}(R) = \tilde{\mathbf{P}}_4 \tilde{\mathbf{P}}_2^{-1}$ . Combining equations (55) and (56) we deduce that the propagator over a T-junction is given by

$$\mathbf{P}(X_2, X_1) = \begin{bmatrix} \mathbf{I}_{4 \times 4} & \mathbf{0}_{4 \times 4} \\ \tilde{\mathbf{Y}} & \mathbf{I}_{4 \times 4} \end{bmatrix}. \tag{57}$$

The S-matrix method is essential for dealing with high frequencies. It can be shown for the T-junction shown in Figure 2, that

$$\begin{bmatrix} \mathbf{u}_{(2)}^{t} \\ \mathbf{u}_{(3)}^{t} \\ \mathbf{u}_{(1)}^{b} \end{bmatrix} = \begin{bmatrix} \mathbf{T}_{(21)} & \mathbf{R}_{(22)} & \mathbf{T}_{(23)} \\ \mathbf{T}_{(31)} & \mathbf{T}_{(32)} & \mathbf{R}_{(33)} \\ \mathbf{R}_{(11)} & \mathbf{T}_{(12)} & \mathbf{T}_{(13)} \end{bmatrix} \begin{bmatrix} \mathbf{u}_{(1)}^{t} \\ \mathbf{u}_{(2)}^{b} \\ \mathbf{u}_{(3)}^{b} \end{bmatrix},$$
(58)

where  $\mathbf{T}_{(ij)}$ ,  $\mathbf{R}_{(ij)}$ , i, j = 1, 2, 3, 4, are given in Appendix E. Define a "wave impedance" matrix  $\tilde{\mathbf{Y}}'$ , which relates the ingoing and outgoing waves at a point:

$$\tilde{\mathbf{u}}^o = \tilde{\mathbf{Y}}' \tilde{\mathbf{u}}^i. \tag{59}$$

Then, substituting it into equation (58), we obtain

$$\begin{bmatrix} \mathbf{u}_{(2)}^f \\ \mathbf{u}_{(1)}^b \end{bmatrix} = \mathbf{S} \begin{bmatrix} \mathbf{u}_{(1)}^f \\ \mathbf{u}_{(2)}^b \end{bmatrix},$$

where the submatrices of S for the T-junction are

$$\mathbf{S}_{1} = \mathbf{T}_{(21)} + \mathbf{T}_{(23)} \tilde{\mathbf{Y}}'(R) [\mathbf{I} - \mathbf{R}_{(33)} \tilde{\mathbf{Y}}'(R)]^{-1} \mathbf{T}_{(31)}, \tag{60a}$$

$$\mathbf{S}_{2} = \mathbf{R}_{(22)} + \mathbf{T}_{(23)} \tilde{\mathbf{Y}}'(R) [\mathbf{I} - \mathbf{R}_{(33)} \tilde{\mathbf{Y}}'(R)]^{-1} \mathbf{T}_{(32)}, \tag{60b}$$

$$\mathbf{S}_{3} = \mathbf{R}_{(11)} + \mathbf{T}_{(13)}\tilde{\mathbf{Y}}'(R)[\mathbf{I} - \mathbf{R}_{(33)}\tilde{\mathbf{Y}}'(R)]^{-1}\mathbf{T}_{(31)}, \tag{60c}$$

$$\mathbf{S}_4 = \mathbf{T}_{(12)} + \mathbf{T}_{(13)} \tilde{\mathbf{Y}}'(R) [\mathbf{I} - \mathbf{R}_{(33)} \tilde{\mathbf{Y}}'(R)]^{-1} \mathbf{T}_{(32)}. \tag{60d}$$

It follows from equation (52) that the "wave impedance"  $\tilde{\mathbf{Y}}'$  can be "propagated" from r to R by

$$\tilde{\mathbf{Y}}'(R) = \tilde{\mathbf{S}}'\tilde{\mathbf{Y}}'(r)\tilde{\mathbf{S}}',\tag{61}$$

where  $\tilde{\mathbf{S}}'$  is given in equation (53), and  $\tilde{\mathbf{Y}}'$  and  $\tilde{\mathbf{Y}}$  are related by

$$\tilde{\mathbf{Y}}' = (\tilde{\mathbf{Y}}\tilde{\mathbf{E}}_1 - \tilde{\mathbf{E}}_3)^{-1}(\tilde{\mathbf{E}}_4 - \tilde{\mathbf{Y}}\tilde{\mathbf{E}}_2), \qquad \tilde{\mathbf{Y}} = (\tilde{\mathbf{E}}_3\tilde{\mathbf{Y}}' + \tilde{\mathbf{E}}_4)(\tilde{\mathbf{E}}_1\tilde{\mathbf{Y}}' + \tilde{\mathbf{E}}_2)^{-1}.$$
 (62a, b)

Note that  $\tilde{\mathbf{Y}}$  and  $\tilde{\mathbf{Y}}'$  should both be evaluated at the same position on the plate.

In summary, the procedure for computing **S** is as follows: (i) assuming that the inner impedance  $\tilde{\mathbf{Y}}(r)$  is known, we first obtain  $\tilde{\mathbf{Y}}'(r)$  from equation (62a); then (ii) "propagate"  $\tilde{\mathbf{Y}}'$  from r to R using equation (61), to obtain  $\tilde{\mathbf{Y}}'(R)$ ; and, finally, (iii) the **S**-matrix follows from equations (60a)–(60d).

# 5.3. T-JUNCTION OF A CYLINDER AND AN INTERNAL SOLID CIRCULAR PLATE In this case, the impedance matrix defined in equation (56) is given by

$$\tilde{\mathbf{Y}}(R) = \mathbf{L} \begin{bmatrix} \tilde{\mathbf{Y}}_f(R) & \mathbf{0} \\ \mathbf{0} & \tilde{\mathbf{Y}}_m(R) \end{bmatrix} \mathbf{G},\tag{63}$$

where  $\tilde{\mathbf{Y}}_f(R)$  and  $\tilde{\mathbf{Y}}_m(R)$  are derived in the Appendix D. All the elements of  $\mathbf{G}_{8\times 8}$  and  $\mathbf{L}_{8\times 8}$  vanish except for  $l_{12}=l_{23}=1$ ,  $l_{34}=l_{41}=-1$  and  $g_{11}=g_{42}=1$ ,  $l_{33}=l_{24}=-1$ . The "wave impedance"  $\tilde{\mathbf{Y}}'(R)$  then may be found using equation (62a) and the S-matrix from equations (60a)–(60d).

#### 6. APPLICATIONS TO CYLINDERS WITH INTERNAL MEMBERS

The methods developed in this paper can be applied to study waves in cylindrical shells with finite regions of material discontinuity and/or stiffeners. Numerous papers have been published on the latter subject. A few of them are concerned with the deformation of the stiffener cross-sections; for example, Hodges *et al.* [43] allows the symmetric stiffeners to suffer cross-sectional distortion, but their method is also a low frequency approximation. Even so, they have shown that the deformation significantly influences the wave propagation characteristics at low frequencies. Accorsi and Bennett [44] considered the cross-sectional deformation using a finite element based technique. The natural and comprehensive way to investigate the effects of the stiffeners is to consider the waves within them. The method presented in this paper is suitable for this purpose.

#### 6.1. THE INTERNAL T-FRAME STRUCTURE

The geometry is shown in Figure 3. In order to deduce the S-matrix, we first need to find the impedance matrix. First note that the forces and velocities at the bottom junction are related according to  $\mathbf{Z}^{(f)}(X_j) = \mathbf{Y}(X_j)\mathbf{Z}^{(g)}(X_j)$ , where j=2 or j=3, and  $\mathbf{Y}(X_2) = \mathbf{P}_3(X_2, X_1)\mathbf{P}_1^{-1}(X_2, X_1)$ ,  $\mathbf{Y}(X_3) = \mathbf{P}_3(X_3, X_4)\mathbf{P}_1^{-1}(X_3, X_4)$ . It then follows from equation (55) that the impedance matrix for the lower T-junction is  $\mathbf{Y}(X_2) - \mathbf{Y}(X_3)$ . Therefore, the impedance matrix for the entire T-frame (see equation (56)) is

$$\tilde{\mathbf{Y}}(R) = [\tilde{\mathbf{P}}_3 + \tilde{\mathbf{P}}_4(\mathbf{Y}(X_2) - \mathbf{Y}(X_3))][\tilde{\mathbf{P}}_1 + \tilde{\mathbf{P}}_2(\mathbf{Y}(X_2) - \mathbf{Y}(X_3))]^{-1}.$$
 (64)

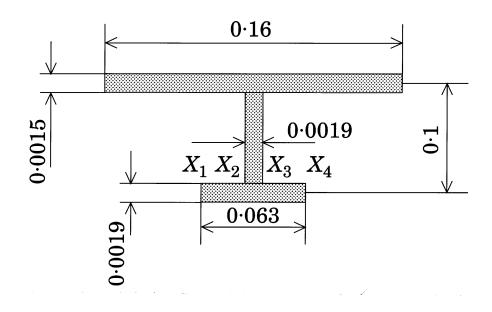


Figure 3. The geometry of an internal T-frame. The numbers indicate the relative dimensions used in the numerical results discussed in section 6.

(66d)

The S-matrix is found by first defining, by analogy with equation (59), a "wave impedance" matrix  $\mathbf{Y}'$  such that  $\mathbf{u}^f = \mathbf{Y}'\mathbf{u}^b$ . It satsifies

$$Y'(X_2) = S'Y'(X_1)S', Y'^{-1}(X_3) = S'Y'^{-1}(X_4)S',$$

where S' is given in equation (22) and also, analogous to equation (62b),

$$\mathbf{Y}(X_2) = [\mathbf{E}_3 \mathbf{Y}'(X_2) + \mathbf{E}_4][\mathbf{E}_1 \mathbf{Y}'(X_2) + \mathbf{E}_2]^{-1},$$
  
$$\mathbf{Y}(X_3) = [\mathbf{E}_3 + \mathbf{E}_4 \mathbf{Y}'^{-1}(X_3)][\mathbf{E}_1 + \mathbf{E}_2 \mathbf{Y}'^{-1}(X_3)]^{-1}.$$

Therefore, the matrix  $\tilde{\mathbf{Y}}'$  of equation (59) follows from the continuity conditions and equation (62a) as

$$\tilde{\mathbf{Y}}'(r) = [(\mathbf{Y}(X_2) - \mathbf{Y}(X_3))\tilde{\mathbf{E}}_1 - \tilde{\mathbf{E}}_3]^{-1}[\tilde{\mathbf{E}}_4 - (\mathbf{Y}(X_2) - \mathbf{Y}(X_3))\tilde{\mathbf{E}}_2]. \tag{65}$$

Finally, the S-matrix is obtained from equations (60a)–(60d) and (61).

#### 6.2. WAVES THROUGH AN INTERNAL BOX STRUCTURE

We consider the box frame stiffener shown in Figure 4 as an example of a substructure which is relatively complex, but still amenable to the methods proposed in this paper. The propagator matrices  $\mathbf{P}^{c_2}$  and  $\mathbf{P}^{c_3}$  depend upon the propagator matrices for each and every section of the box,

$$\mathbf{P}^{C_2} = \mathbf{P}(X_4, X_2), \quad \mathbf{P}^{C_3} = \mathbf{\tilde{P}}(x_5, x_{10})\mathbf{P}(X_9, X_8)\mathbf{K}\mathbf{\tilde{P}}(x_7, x_3),$$

where **K** is given in equation (28). Following the procedure of Appendix A and noticing the directions of the forces at the joints (see the first of equation (55)) we can find the propagator matrix  $P(X_6, X_1)$ . The submatrices of  $P(X_6, X_1)$  are

$$\begin{aligned} \mathbf{P}_{1} &= \mathbf{P}_{1}^{C_{2}} + \mathbf{P}_{2}^{C_{2}} (\mathbf{P}_{2}^{C_{3}} - \mathbf{P}_{2}^{C_{2}})^{-1} (\mathbf{P}_{1}^{C_{2}} - \mathbf{P}_{1}^{C_{3}}), \qquad \mathbf{P}_{2} &= \mathbf{P}_{2}^{C_{2}} (\mathbf{P}_{2}^{C_{3}} - \mathbf{P}_{2}^{C_{2}})^{-1} \mathbf{P}_{2}^{C_{3}}, \quad (66a, b) \\ \mathbf{P}_{3} &= \mathbf{P}_{3}^{C_{3}} + \mathbf{P}_{3}^{C_{2}} + \mathbf{P}_{4}^{C_{3}} (\mathbf{P}_{2}^{C_{3}})^{-1} (\mathbf{P}_{1}^{C_{2}} - \mathbf{P}_{1}^{C_{3}}) \\ &+ (\mathbf{P}_{4}^{C_{2}} + \mathbf{P}_{4}^{C_{3}} (\mathbf{P}_{2}^{C_{3}})^{-1} \mathbf{P}_{2}^{C_{2}}) (\mathbf{P}_{2}^{C_{3}} - \mathbf{P}_{2}^{C_{2}})^{-1} (\mathbf{P}_{1}^{C_{2}} - \mathbf{P}_{1}^{C_{3}}), \quad (66c) \end{aligned}$$

The multi-channel S-matrix presented in section 2 is again preferable for high frequencies. It is observed that equation (54) should be employed for the left plate  $(x_3, x_7)$ , while equation (52) applies to the right plate  $(x_{10}, x_5)$ . The wave propagators for the two joints  $(X_8, x_7)$  and  $(x_{10}, X_9)$  are  $\mathbf{Q}(X_8, x_7) = \mathbf{E}^{-1}(X_8)\mathbf{K}\mathbf{\tilde{E}}(x_7)$  and  $\mathbf{Q}(x_{10}, X_9) = \mathbf{\tilde{E}}'^{-1}(x_{10})\mathbf{E}(X_9)$ , where  $\mathbf{K}$  is given in equation (28), from which the S-matrices for the joints can be obtained. Then the S-matrix for the wave channel  $(x_3, x_5)$  follows from those for

 $\mathbf{P}_{4} = (\mathbf{P}_{4}^{C_{2}} + \mathbf{P}_{4}^{C_{3}}(\mathbf{P}_{2}^{C_{3}})^{-1}\mathbf{P}_{2}^{C_{2}})(\mathbf{P}_{2}^{C_{3}} - \mathbf{P}_{2}^{C_{2}})^{-1}\mathbf{P}_{2}^{C_{3}}.$ 

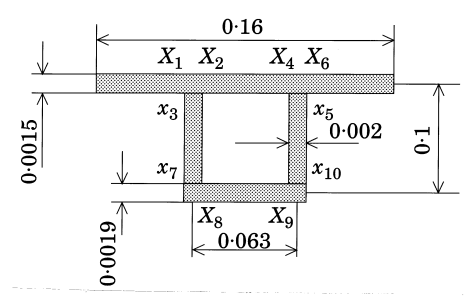


Figure 4. The geometry and dimensions of an internal box frame.

the plates, the junctions, the inner cylinder and the addition rule. Finally, the S-matrix for the box is obtained from equations (35)–(40).

#### 6.3. NUMERICAL RESULTS FOR PERIODIC STIFFENERS

The frequency dependent behavior of periodic cylinders can be revealed by solving the eigenvalue problems of equations (14) and (15). It is observed that there are eight complex propagation constants, four of them negative counterparts of the other four. The positive real and imaginary parts of the propagation constants for three different examples are shown in Figures 5–7. In all three examples the stiffeners and the cylinder are made of the same material and, hence, the form of the dispersion curves depends only on the Poisson ratio *v* and the dimensions of the periodically stiffened cylinder normalized relative to the radius of the cylinder. The natural unit of frequency is the ring frequency, and all results are shown in these units. The final example described below was the most numerically time consuming. The curves in Figure 7 required about 80 s CPU time on a SPARC 4 workstation.

The first example, which is the same as that considered by Mead and Bardell [45], is a cylinder with periodic exterior stiffeners. The dispersion curves computed from equation (15) are shown in Figure 5, and are consistent with those obtained by Mead and Bardell [45] using a different method. The agreement is particularly good at low frequencies, but very small differences are apparent at higher frequencies, which can be attributed to the different models used here and by Mead and Bardell [45].

The second example is a cylinder with periodic internal T-frames. The physical dimensions of the basic period are given in Figure 3, where the units are normalized relative to the outer radius of the cylinder. The computed dispersion curves are shown in Figure 6 for circumferential wavenumber n = 4 and v = 0.3. We note that there are only four small passing bands in the frequency range  $0.0 \le \Omega \le 2.0$ , but there is a large passing band for

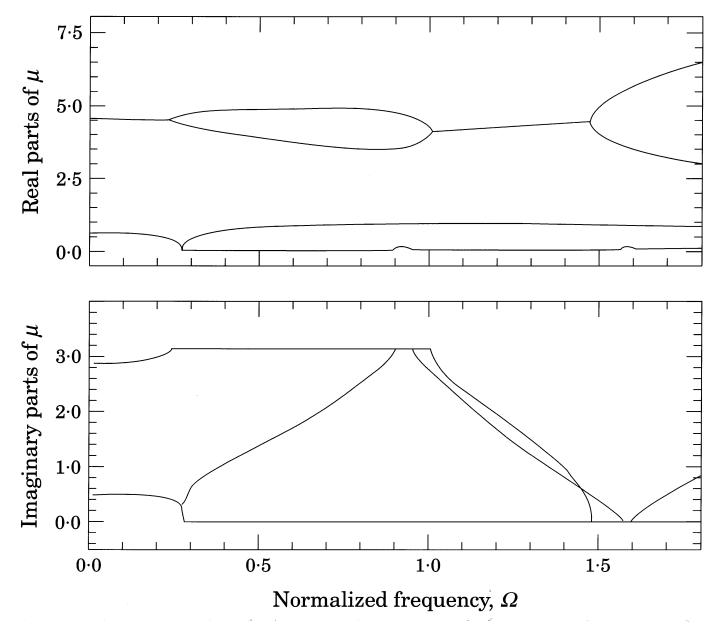


Figure 5. Dispersion curves for the periodic stiffened cylinder model of Mead and Bardell [45], with n = 5 and v = 0.3. The thickness, periodic length, rib thickness and rib height are  $1.15 \times 10^{-2}$ , 0.303,  $2.10 \times 10^{-2}$  and  $5.62 \times 10^{-2}$ , respectively, all relative to the radius. Precise details of the geometry and the dimensions are given in Fig. 5 of reference [45]. The curves shown here correspond to Figure 6(a) in reference [45].

WAVES IN SHELLS 475

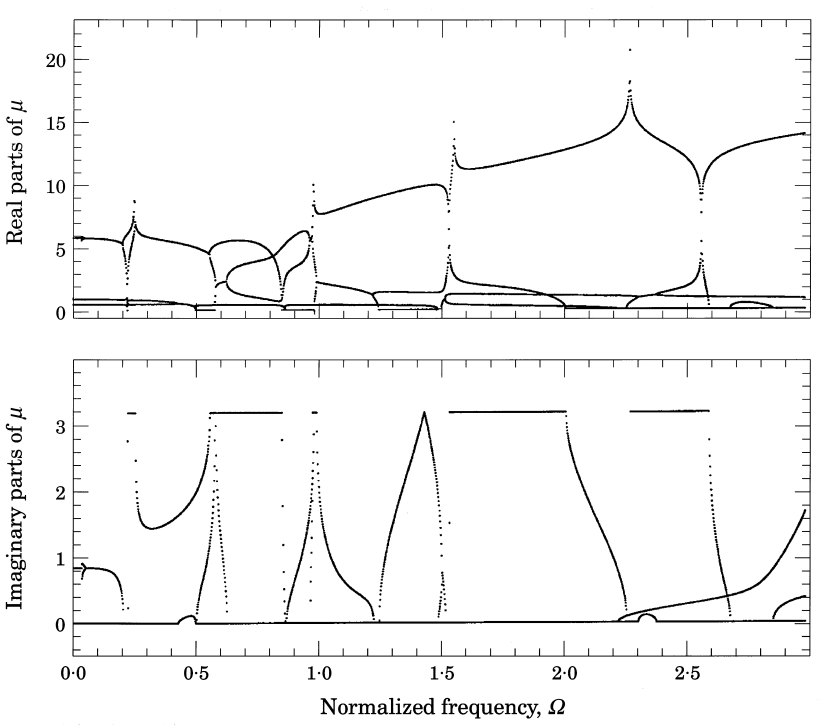


Figure 6. Dispersion curves for the cylindrical shell with periodic internal T-frames, with dimensions as shown in Figure 3. Also, n = 4 and v = 0.3.

 $\Omega \geqslant 2.02$ . The final example illustrates the multi-channel S-matrix approach. Dispersion curves for a cylinder with periodic box stiffeners as shown in Figure 4 are presented in Figure 7 for n=2 and v=0.3.

# 7. SUMMARY

The propagator matrix and the S-matrix offer two equally valid but alternative methods for studying the vibration of structures. The S-matrix approach has been emphasized in this paper because it does not suffer from numerical instabilities at higher frequencies, in contrast to the propagator matrix which contains elements that become exponentially unbounded with increasing frequency. Explicit and useful expressions have been derived for the S-matrices of the basic elements of a complex structure: a uniform section, multi-channel regions, and joints. Addition rules for the S-matrix are also given. We have demonstrated how these separate elements may be combined to study wave propagation on cylindrical shells with material or structural discontinuity in the axial direction, and with internal wave-bearing attachments. The same methods can be applied to structures with far greater complexity by suitably cascading S-matrices for substructures.

We note that in order to obtain the S-matrix, the matrix  $\mathbf{Q}_4$  needs to be inverted. The S-matrix approach fails when  $\mathbf{Q}_4$  is singular. This happens for a plate-shell junction most probably when the azimuthal number n is small, or "normal incidence" onto the junction, although the S-matrix approach works well for the plates, and also for the shells, even for n=0. However, the propagator matrix method can be employed for a small region near the junction where  $\mathbf{Q}_4$  is singular, so that there is no numerical instability, while the S-matrix approach is used for other parts of the structure.

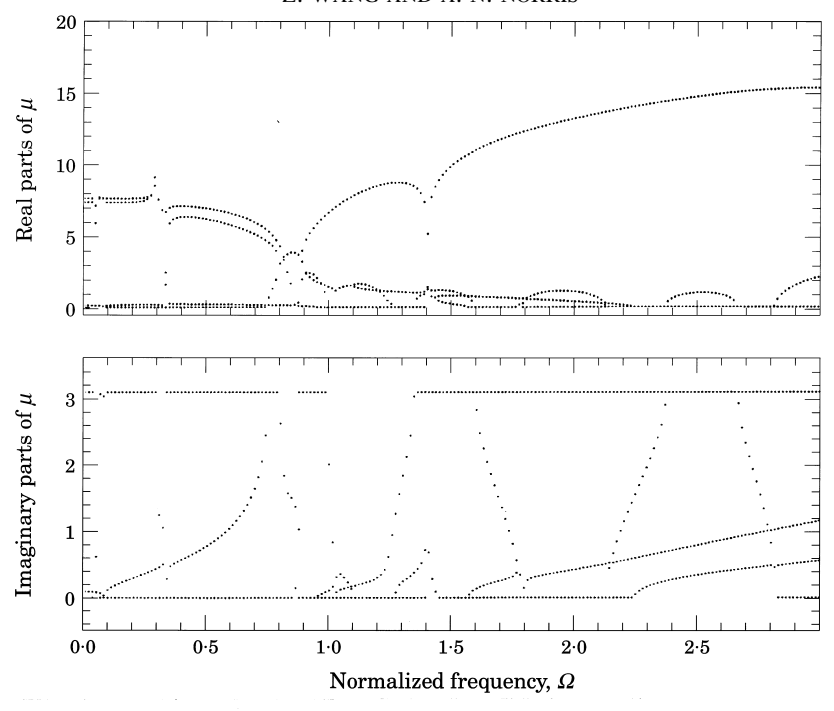


Figure 7. Dispersion curves for the cylindrical shell with periodic internal box stiffeners (see Figure 4) and n = 2, v = 0.3.

At the end of this paper, we would like to point out that the S-matrix approach can be employed whenever the S-matrix, or the asymptotic S-matrix, exist—and that it is preferred for high frequencies.

# ACKNOWLEDGMENT

This work was supported by the United States Office of Naval Research.

#### REFERENCES

- 1. W. T. THOMSON 1950 *Journal of Applied Physics* 21, 89–93. Transmission of elastic waves through a stratified solid medium.
- 2. N. A. HASKELL 1953 *Bulletin of the Seismological Society of America* **43**, 17–34. The dispersion of surface waves on multilayered media.
- 3. Y. K. LIN and B. K. Donaldson 1969 *Journal of Sound and Vibration* 10, 103–143. A brief survey of transfer matrix technique with special reference to the analysis of aircraft panels.
- 4. L. Knopoff 1964 *Bulletin of the Seismological Society of America* **54**, 431–438. A matrix method for elastic wave problems.
- J. W. Dunkin 1965 Bulletin of the Seismological Society of America 55, 335–358. Computation of modal solution in layered elastic media at high frequencies.
- B. L. N. Kennett 1983 Seismic Wave Propagation in Stratified Media. Cambridge: Cambridge University Press.
- 7. B. L. N. Kennett 1974 Bulletin of the Seismological Society of America **64**, 1685–1696. Reflection, rays and reverberations.
- 8. B. L. N. Kennett and N. J. Kerry 1979 *Geophysical Journal of the Royal Astronomical Society* 57, 557–583. Seismic waves in a stratified half space.

- R. Redheffer 1961 Modern Mathematics for Engineers. New York: McGraw-Hill. See Chapter 12.
- Y. Yong and Y. K. Lin 1990 American Institute of Aeronautics and Astronautics Journal 28, 1250–1258. Dynamic of complex truss-type space structures.
- 11. Y. Yong and Y. K. Lin 1992 *Journal of Sound and Vibration* **156**, 27–45. Dynamic response analysis of truss-type structural networks: a wave propagation approach.
- 12. A. H. Von Flotow 1986 *Journal of Sound and Vibration* **106**, 433–450. Disturbance propagation in structural networks.
- 13. B. R. Mace 1984 *Journal of Sound and Vibration* 197, 237–246. Wave reflection and transmission in beams.
- 14. M. S. TAVAKOLI and R. SINGH 1989 *Journal of Sound and Vibration* 100, 97–123. Eigensolutions of joined/hermetic shell structures using the space method.
- 15. M. S. TAVAKOLI and R. SINGH 1990 *Journal of Sound and Vibration* **136**, 141–145. Modal analysis of a hermetic can.
- 16. A. Kalnins 1964 *Journal of the Acoustical Society of America* **36**, 1355–1356. Free vibration of rotationally symmetric shells.
- 17. Y. Yu 1958 *Journal of Aerospace Science* **25**, 699–715. Vibrations of thin cylindrical shells analyzed by means of Donnell-type equations.
- 18. A. Norris and Z. Wang 1993 *Journal of Sound and Vibration* 169, 485-502. Low frequency bending waves in periodic plates.
- 19. G. V. Borgiotti and E. M. Rosen 1992 *Journal of the Acoustical Society of America* **91**, 991–925. The state vector approach to the wave and power flow analysis of the forced vibrations of a cylindrical shell, part I: Infinite cylinder in vacuum.
- 20. G. V. Borgiotti and E. M. Rosen 1993 *Journal of the Acoustical Society of America* **93**, 864–874. The state vector approach to the wave analysis of the forced vibration of a cylindrical shell, part II: finite cylinders in vacuum.
- 21. T. IRIE, G. YAMADA and Y. KOBAYASHI 1984 *Journal of Sound and Vibration* **96**, 133–142. Free vibration of non-circular cylindrical shell with longitudinal interior partitions.
- 22. L. Brillouin 1953 Wave Propagation in Periodic Structures. New York: Dover.
- 23. A. K. Roy and R. Plunkett 1986 *Journal of Sound and Vibration* 104, 395–410. Wave attenuation in periodic structures.
- 24. I. MIRSKY and G. HERMANN 1958 *Journal of Applied Mechanics* 25, 97–103. Axially symmetric motions of thick cylindrical shells.
- 25. I. Mirsky and G. Hermann 1957 *Journal of the Acoustical Society of America* **29**, 116–123. Nonaxially symmetric motions of cylindrical shells.
- 26. Y. Yong and Y. K. Lin 1989 *Journal of Sound and Vibration* 129, 99–118. Propagation of decaying waves in periodic and piecewise periodic structures of finite length.
- A. D. Pierce 1989 Elastic Wave Propagation, Proceedings of the second I.U.T.A.M.-I.U.P.A.P.
   Symposium on Elastic Wave Propagation (M. F. McCarthy and M. A. Hayes, editors)
   205–210. Amsterdam: North-Holland. Wave propagation on thin-walled elastic cylindrical
   shells.
- 28. A. E. H. Love 1944 A Treatise on the Mathematical Theory of Elasticity. New York: Dover.
- 29. L. Cremer, M. Heckl and E. E. Ungar 1980 Structure-borne Sound. Berlin: Springer-Verlag.
- 30. V. A. Veshev and D. P. Kouzov 1977 *Soviet Physics—Acoustics* **23**, 206–211. Influence of the medium on the vibration of plates joined at right angles.
- 31. V. N. Romanov 1969 *Soviet Physics—Acoustics* **15**, 234–240. Investigation of a plate T-junction in a diffuse flexural wave field.
- 32. S. V. Budrin and A. S. Nikiforov 1964 Soviet Physics—Acoustics 9, 333–336. Wave transmission through assorted plate joints.
- 33. I. T. Lu, H. L. Bertoni and H. Y. Chen 1992 *Journal of the Acoustic Society of America* **92**, 510–526. Coupling of plate modes at joints.
- 34. B. L. SMITH and E. E. HAFT 1967 American Institute of Aeronautic and Astronautics Journal 5, 2080–2082. Vibration of a cylindrical shell closed by an elastic plate.
- 35. B. L. SMITH 1966 *Ph.D. Thesis*, *Kansas State University*. Free vibration of cylindrical shells of finite length.
- 36. Y. HIRANO 1969 Bulletin of the Japan Society of Mechanical Engineering 12, 459–469. Axisymmetric vibrations of thin drums.
- 37. S. TAKAHASHI and Y. HIRANO 1970 *Bulletin of the Japan Society of Mechanical Engineering* 13, 240–247. Vibration of a combination of circular plates and cylindrical shells (1st report, a cylindrical shell with circular plates at ends).

- 38. T. IRIE, G. YAMADA and H. IDA 1985 *Journal of Sound and Vibration* **96**, 133–142. Free vibration of longitudinally stiffened prismatic shell with and without partitions.
- 39. Y. Kobayashi and T. Irie 1987 *Journal of the Acoustical Society of America* **81**, 1795–1800. Free vibration of unsymmetrically jointed shell structures with a closed member.
- L. CHENG and J. NICOLAS 1992 Journal of Sound and Vibration 155, 231–247. Free vibration analysis of a cylindrical shell-circular plate system with general coupling and various boundary conditions.
- 41. L. L. FAULKNER 1969 *Thesis*, *Purdue University*, Vibration analysis of shell structures using receptances.
- 42. D. T. Huang and W. Soedel 1993 *Journal of Sound and Vibration* **162**, 403–427. Natural frequencies and modes of a circular plate welded to a circular cylindrical shell at arbitrary axial positions.
- 43. C. H. Hodges, J. Power and J. Woodhouse 1985 *Journal of Sound and Vibration* **101**, 219–235. The low frequency vibration of a ribbed cylinder, part I: theory.
- 44. M. L. Accorsi and M. S. Bennett 1991 *Journal of Sound and Vibration* 148, 279–292. A finite element based method for the analysis of free wave propagation in stiffened cylinders.
- 45. D. J. MEAD and N. S. BARDELL 1986 *Journal of Sound and Vibration* 115, 499–520. Free vibration of a thin cylindrical shell with periodic circumferential stiffeners.
- 46. S. TIMOSHENKO 1959 Theory of Plates and Shells. New York: McGraw-Hill.
- 47. G. N. WATSON 1929 A Treatise on the Theory of Bessel Functions. London: Cambridge University press, first edition.

#### APPENDIX A: THE MULTI-CHANNEL PROPAGATOR MATRIX

The concatenation rule for propagators will be illustrated by way of considering the example structure in Figure 1. We first write

$$\mathbf{Z}(X_{l-1+i}) = \mathbf{P}^{c_i} \mathbf{Z}(X_i), \qquad i = 2, ..., l,$$
 (A1)

where  $\mathbf{P}^{C_i}$ , i = 2,..., l, is the propagator matrix for channel i, respectively. Equation (A1) together with the velocity continuity conditions at both the left and right joints, which follow from equation (34), implies that

$$\mathbf{Z}^{(f)}(X_i) = \mathbf{A}_i \mathbf{Z}^{(v)}(X_1) + \mathbf{B}_i \mathbf{Z}^{(f)}(X_2), \qquad i = 3, ..., l,$$
(A2)

where  $\mathbf{A}_i = (\mathbf{P}_2^{C_i})^{-1}(\mathbf{P}_1^{C_i} - \mathbf{P}_1^{C_i})$ , and  $\mathbf{B}_i = (\mathbf{P}_2^{C_i})^{-1}\mathbf{P}_2^{C_2}$ , i = 3,..., l. Substituting the force vectors from equation (A2) into the force continuity condition for the left joint, from equation (34), we obtain

$$\begin{bmatrix} \mathbf{Z}^{(v)}(X_2) \\ \mathbf{Z}^{(f)}(X_2) \end{bmatrix} = \begin{bmatrix} \mathbf{I} & \mathbf{0} \\ -\left(\mathbf{I} + \sum_{i=3}^{l} \mathbf{B}_i\right)^{-1} \sum_{i=3}^{l} \mathbf{A}_i & -\left(\mathbf{I} + \sum_{i=3}^{l} \mathbf{B}_i\right)^{-1} \end{bmatrix} \begin{bmatrix} \mathbf{Z}^{(v)}(X_1) \\ \mathbf{Z}^{(f)}(X_1) \end{bmatrix}, \tag{A3}$$

whereas substitution of equation (A2) into equation (A1) gives

$$\begin{bmatrix} \mathbf{Z}^{(t)}(X_{l-1+i}) \\ \mathbf{Z}^{(t)}(X_{l-1+i}) \end{bmatrix} = \begin{bmatrix} \mathbf{P}_{1}^{C_{2}} & \mathbf{P}_{2}^{C_{2}} \\ \mathbf{P}_{3}^{C_{1}} + \mathbf{P}_{4}^{C_{1}}\mathbf{A}_{i} & \mathbf{P}_{4}^{C_{1}}\mathbf{B}_{i} \end{bmatrix} \begin{bmatrix} \mathbf{Z}^{(t)}(X_{2}) \\ \mathbf{Z}^{(t)}(X_{2}) \end{bmatrix}, \qquad i = 3, ..., l.$$
(A4)

These relations allow us to show, using the force continuity condition for the right joint, that

$$\begin{bmatrix} \mathbf{Z}^{(v)}(X_{2l}) \\ \mathbf{Z}^{(f)}(X_{2l}) \end{bmatrix} = \begin{bmatrix} \mathbf{P}_1^{C_2} & \mathbf{P}_2^{C_2} \\ -\mathbf{P}_3^{C_3} - \sum_{i=3}^{l} (\mathbf{P}_3^{C_i} + \mathbf{P}_4^{C_i} \mathbf{A}_i) & -\mathbf{P}_4^{C_2} - \sum_{i=3}^{l} \mathbf{P}_4^{C_i} \mathbf{B}_i \end{bmatrix} \begin{bmatrix} \mathbf{Z}^{(v)}(X_2) \\ \mathbf{Z}^{(f)}(X_2) \end{bmatrix}.$$

Finally, combining this identity with equation (A3) results in

$$\mathbf{Z}(X_{2l}) = \mathbf{P}(X_{2l}, X_1)\mathbf{Z}(X_1), \tag{A5}$$

where  $\mathbf{P}$  is the propagator for the multi-channel element, with submatrices (see equation (11))

$$\mathbf{P}_{1} = \mathbf{P}_{1}^{C_{2}} - \mathbf{P}_{2}^{C_{2}} \left( \mathbf{I} + \sum_{i=3}^{l} \mathbf{B}_{i} \right)^{-1} \sum_{i=3}^{l} \mathbf{A}_{i}, \qquad \mathbf{P}_{2} = -\mathbf{P}_{2}^{C_{2}} \left( \mathbf{I} + \sum_{i=3}^{l} \mathbf{B}_{i} \right)^{-1}, \qquad (A6a, b)$$

$$\mathbf{P}_{3} = -\mathbf{P}_{3}^{C_{2}} - \sum_{i=3}^{l} (\mathbf{P}_{3}^{C_{i}} + \mathbf{P}_{4}^{C_{i}} \mathbf{A}_{i}) + \left(\mathbf{P}_{4}^{C_{2}} + \sum_{i=3}^{l} \mathbf{P}_{4}^{C_{i}} \mathbf{B}_{i}\right) \left(\mathbf{I} + \sum_{i=3}^{l} \mathbf{B}_{i}\right)^{-1} \sum_{2}^{l} \mathbf{A}_{i}, \quad (A6c)$$

$$\mathbf{P}_4 = \left(\mathbf{P}_4^{C_2} + \sum_{i=3}^{l} \mathbf{P}_4^{C_i} \mathbf{B}_i\right) \left(\mathbf{I} + \sum_{i=3}^{l} \mathbf{B}_i\right)^{-1}.$$
 (A6d)

# APPENDIX B: EQUATIONS OF MOTION FOR CYLINDRICAL SHELLS

The equations of motion of a cylindrical shell used here are derived from the static equilibrium equations in Timoshenko [46]. Adding the dynamic terms, we have

$$R\frac{\partial N_X}{\partial X} + \frac{\partial N_{\phi X}}{\partial \varphi} + Rf_X = R\rho h \frac{\partial^2 U}{\partial t^2},$$
 (B7a)

$$\frac{\partial N_{\varphi}}{\partial \varphi} + R \frac{\partial N_{X\varphi}}{\partial X} - Q_{\varphi} + R f_{\varphi} = R \rho h \frac{\partial^{2} V}{\partial t^{2}}, \tag{B7b}$$

$$-R\frac{\partial Q_X}{\partial X} - \frac{\partial Q_{\varphi}}{\partial \varphi} - N_{\varphi} - (p_+ - p_-)R + Rf_R = R\rho h \frac{\partial^2 W}{\partial t^2},$$
 (B7c)

$$R\frac{\partial M_{X\varphi}}{\partial X} - \frac{\partial M_{\varphi}}{\partial \varphi} + RQ_{\varphi} = 0, \tag{B7d}$$

$$\frac{\partial M_{\varphi X}}{\partial \omega} + R \frac{\partial M_X}{\partial X} - RQ_X = 0, \tag{B7e}$$

where  $\rho$ , h and R are the mass density, the thickness and the radius of the shell, respectively. U, V and W measure the displacements of the middle plane of the shell in the axial direction X, the circumferential direction  $\varphi$  and the radial direction, respectively;  $N_X, \ldots, Q_X, \ldots$  are resultant forces and  $M_X, \ldots$  are resultant moments;  $p_+$  and  $p_-$  are the pressures exerted externally and internally by the fluid loading; and  $\mathbf{f}$  is the applied force. We also have the constitutive relations

$$N_{X} = C \left( \frac{\partial U}{\partial X} + v \frac{\partial V}{R \partial \varphi} + v \frac{W}{R} \right), \qquad N_{\varphi} = C \left( v \frac{\partial U}{\partial X} + \frac{\partial V}{R \partial \varphi} + \frac{W}{R} \right), \qquad (B8a, b)$$

$$N_{X\varphi} = N_{\varphi X} = \frac{(1-v)}{2} C \left( \frac{\partial U}{R \partial \varphi} + \frac{\partial V}{\partial X} \right),$$
 (B8c)

$$M_{X} = -D\left(v\frac{\partial V}{R^{2}\partial\varphi} - \frac{\partial^{2}W}{\partial X^{2}} - v\frac{\partial^{2}W}{R^{2}\partial\varphi^{2}}\right), \qquad M_{\varphi} = -D\left(\frac{\partial V}{R^{2}\partial\varphi} - v\frac{\partial^{2}W}{\partial X^{2}} - \frac{\partial^{2}W}{R^{2}\partial\varphi^{2}}\right),$$
(B8d, e)

$$M_{X\varphi} = -M_{\varphi X} = (1 - v) \frac{D}{R} \left( \frac{\partial V}{\partial X} - \frac{\partial^2 W}{\partial X \partial \varphi} \right),$$
 (B8f)

where the bending and extensional stiffness are  $D = Eh^3/12(1 - v^2)$  and  $C = Eh/(1 - v^2)$ , and E and v are the Young's modulus and Poisson ratio, respectively. The results reported

in this paper are for shells *in vacuo*, although they could be generalized to include exterior fluid loading by using a local impedance relation of the form  $p_+ - p_- = -i\omega Z_{rad}W$ , where  $Z_{rad}$  is the specific radiation impedance.

Substituting the constitutive relations into the equations of motion it can be seen that the first terms of the right sides of equations (B8d)–(B8f) and  $Q_{\varphi}$  in equation (B7b) may be neglected when  $h \ll \lambda$  and  $h \ll R$ , where  $\lambda$  is the wavelength (this simplification leads to the Donnell–Yu equations [17]). Ignoring these terms, we obtain

$$\frac{\partial U}{\partial X} = -\frac{v}{R} W - \frac{v}{R} \frac{\partial V}{\partial \varphi} + \frac{1}{C} N_X, \qquad \frac{\partial V}{\partial X} = -\frac{\partial U}{R \partial \varphi} + \frac{2}{(1+v)C} S_X, \qquad \text{(B9a, b)}$$

$$\frac{\partial N_X}{\partial X} = \rho h \frac{\partial^2 U}{\partial t^2} - \frac{\partial S_X}{R \partial \varphi} - f_X, \qquad \frac{\partial S_X}{\partial X} = \rho h \frac{\partial^2 V}{\partial t^2} - \frac{Eh}{R^2} \frac{\partial W}{\partial \varphi} - \frac{Eh}{R^2} \frac{\partial^2 V}{\partial \varphi^2} - v \frac{1}{R} \frac{\partial N_X}{\partial \varphi} - f_{\varphi}, \qquad \text{(B9c, d)}$$

$$\frac{\partial^2 W}{\partial X^2} = -\frac{v}{R^2} \frac{\partial^2 W}{\partial \varphi^2} + \frac{1}{D} M_X, \qquad \frac{\partial T_X}{\partial X} = -\Gamma W - \frac{Eh}{R^2} \frac{\partial V}{\partial \varphi} - v \frac{1}{R^2} \frac{\partial^2 M_X}{\partial \varphi^2} - v \frac{1}{R} N_X + f_R, \qquad \text{(B9e, f)}$$

$$\frac{\partial M_X}{\partial X} = -2D(1-v) \frac{\partial^3 W}{R^2 \partial \varphi^2 \partial X} + T_X, \qquad \text{(B9g)}$$

where

$$\Gamma = \frac{Eh^3}{12R^4} \frac{\partial^4}{\partial \varphi^4} + \frac{Eh}{R^2} + \rho h \frac{\partial^2}{\partial t^2} - i\omega Z_{rad}, \qquad S_X = N_{X\varphi} + \frac{M_{X\varphi}}{R}, \qquad T_X = Q_X - \frac{\partial M_{X\varphi}}{R \partial \varphi}.$$

Justification of the choice of the quantities  $S_X$  and  $T_X$  for static problems can be found in Timoshenko [46]. Eliminating the resultant forces and moments in equations (B9a)–(B9g), we arrive at the Donnell–Yu equations [17].

# APPENDIX C: SOME MATRICES

The force vector in equation (1) is  $\mathbf{F} = (0, 0, 0, 0, -f_{\varphi}, -f_{X}, 0, -f_{R})^{T}$ , and the matrix  $\mathbf{N}$  is

where (see Appendix B)

$$\hat{\Gamma} = -\frac{Eh^3}{12} \frac{n^4}{R^4 \omega} - \frac{Eh}{R^2 \omega} + \rho h \omega + i Z_{rad}, \tag{C11}$$

**G** is an  $8 \times 8$  matrix with all elements zero except  $g_{11} = g_{23} = g_{35} = g_{47} = 1$ ,  $g_{54} = g_{62} = g_{78} = g_{86} = -1$  and, obviously  $\mathbf{G}^{-1} = \mathbf{G}^{\mathsf{T}}$ . The matrices **C**,  $\mathbf{N}_{Mem}$  and  $\mathbf{N}_{Flex}$  in equation (41) can be identified from equations (41) and (C10), and the  $4 \times 4$  matrix  $\mathbf{J}_4$  is  $(J_4)_{ij} = \delta_{i+j,5}$ . The matrices in the simplified  $4 \times 4$  system of equations (43) and (44) are

$$\mathbf{N}_{1} = \begin{bmatrix} -\frac{vn}{R} & \frac{\omega_{r}\Omega}{C} & -i\frac{v}{R} & 0\\ -\frac{Ehn^{2}}{R^{2}\omega_{r}\Omega} + \rho h\omega_{r}\Omega & -\frac{vn}{R} & -i\frac{Ehn}{R^{2}\omega_{r}\Omega} & 0\\ 0 & 0 & i\frac{vn^{2}}{R^{2}} & \frac{\omega_{r}\Omega}{D} \\ i\frac{Ehn}{R^{2}\omega_{r}\Omega} & i\frac{v}{R} & \hat{\Gamma}(\Omega) & -i\frac{vn^{2}}{R^{2}} \end{bmatrix},$$
(C12)

$$\mathbf{N}_{2} = \begin{bmatrix} -\frac{n}{R} & \frac{2\omega_{r}\Omega}{(1-v)C} & 0 & 0\\ \rho h\omega_{r}\Omega & -\frac{n}{R} & 0 & 0\\ 0 & 0 & i & 0\\ 0 & 0 & -2D(1-v)\frac{n^{2}}{R^{2}\omega_{r}\Omega} & -i \end{bmatrix}, \quad (C13)$$

where  $\Omega = \omega/\omega_r$ , and  $\omega_r = R^{-1}\sqrt{E/\rho(1-v^2)}$  is the ring frequency. The product  $N_1N_2$  is

$$\begin{bmatrix} \frac{1}{R^{2}}(vn^{2} + \Omega^{2}) & \frac{n(1+v)^{2}\omega_{r}\Omega}{REh} & \frac{v}{R} & 0\\ \frac{Ehn}{R^{3}\omega_{r}\Omega}\left(n^{2} - \frac{\Omega^{2}}{1-v}\right) & \frac{1}{R^{2}}\left(-(2+v)n^{2} + \frac{2\Omega^{2}}{(1-v)}\right) & \frac{Ehn}{R^{2}\omega_{r}\Omega} & 0\\ 0 & 0 & \frac{1}{R^{2}}(-2+v)n^{2} & -i\frac{\omega_{r}\Omega}{D}\\ i\frac{Eh}{R^{3}\omega_{r}\Omega}\left(-n^{2} + \frac{v\Omega^{2}}{1-v^{2}}\right) & i\frac{1}{R^{2}}(2+v)n & -i\frac{Eh}{R^{2}\omega_{r}\Omega}\left(\frac{(1-v)\beta^{2}n^{4}}{1+v} + 1 - \frac{\Omega^{2}}{1-v^{2}}\right) & -\frac{vn^{2}}{R^{2}} \end{bmatrix}.$$
(C14)

# APPENDIX D: WAVE MATRICES FOR CIRCULAR PLATES

Separate propagator matrices are defined by

$$\mathbf{z}_{\alpha}(r) = \mathbf{P}_{\alpha}(r, R)\mathbf{z}_{\alpha}(R), \qquad \alpha = f \text{ or } m. \tag{D15}$$

It can be shown that, using equations (48a)–(48c),

$$\mathbf{P}_{\alpha}(r,R) = \mathbf{N}_{\alpha}(r)\mathbf{N}_{\alpha}^{-1}(R), \qquad \alpha = f \text{ or } m.$$
 (D16)

For convenience of further development, we write  $N_f$  and  $N_m$  as products of two matrices,

$$\mathbf{N}_{f}(r) = \begin{bmatrix} -\mathbf{i}\omega & 0 & -\mathbf{i}\omega & 0\\ 0 & -\mathrm{i}c\omega & 0 & c\omega\\ -D_{s}\kappa(\mathrm{i}cr) & D_{s}cr & -D_{s}\kappa(cr) & \mathrm{i}D_{s}cr\\ -\frac{D_{s}n^{2}}{r} & \frac{D_{s}}{r}\kappa(cr)cr & -\frac{D_{s}n^{2}}{r} & \mathrm{i}\frac{D_{s}}{r}\kappa(\mathrm{i}cr)cr \end{bmatrix} \mathbf{\Pi}(cr,\mathrm{i}cr), \quad (D17)$$

$$\mathbf{N}_{m}(r) = \begin{bmatrix} 0 & -\mathrm{i}aw & -\mathrm{i}\omega\frac{n}{r} & 0 \\ \omega\frac{n}{r} & 0 & 0 & \omega b \\ -\mathrm{i}C_{s}n & \mathrm{i}C_{s}nar & \mathrm{i}C_{s}\hat{\kappa}(ibr) & -\mathrm{i}C_{s}br \\ C_{s}\kappa(iar) & -C_{s}ar & -C_{s}n & C_{s}nbr \end{bmatrix} \mathbf{\Pi}(ar, br), \tag{D18}$$

where

$$\Pi(x,y) = \begin{bmatrix}
H_n^{(1)}(x) & H_n^{(2)}(x) & 0 & 0 \\
H_n^{(1)'}(x) & H_n^{(2)'}(x) & 0 & 0 \\
0 & 0 & H_n^{(1)}(y) & H_n^{(2)}(y) \\
0 & 0 & H_n^{(1)'}(y) & H_n^{(2)'}(y)
\end{bmatrix} e^{in\varphi}.$$
(D19)

The flexural parameters are  $c^4 = \omega^2 \tilde{\rho} \tilde{h}/\tilde{D}$ ,  $D_s = r^{-2}(1-\tilde{v})\tilde{D}$ , and  $\kappa(x) = n^2 + \frac{x^2}{(1-\tilde{v})}$ ; and the membrane parameters are  $a = \omega/c_p$  and  $b = \omega/c_s$ , where  $c_p = \sqrt{\tilde{C}/\tilde{\rho}}\tilde{h}$  is the longitudinal thin plate velocity and  $c_s = c_p \sqrt{(1-\tilde{v})/2}$  is the shear velocity; also,  $C_s = r^{-2}(1-\tilde{v})\tilde{C}$  and  $\hat{\kappa}(x) = n^2 + \frac{x^2}{2}$ .

Making use of the asymptotic expressions, for  $|z| \gg 1$ ,

$$\frac{H_n^{(1)}(z)}{H_n^{(1)'}(z)} = e^{iz} \begin{cases} \alpha_n(z) & H_n^{(2)}(z) \\ \gamma_n(z), & H_n^{(2)'}(z) \end{cases} = e^{-iz} \begin{cases} \beta_n(z) \\ \delta_n(z), \end{cases}$$
(D20)

where

$$\left. egin{aligned} \left. lpha_n(z) \right\} = \sqrt{rac{2}{\pi z}} \left( \mp \mathrm{i} 
ight)^n \mathrm{e}^{\mp \mathrm{i} \pi/4} (P_n(z) \pm \mathrm{i} Q_n(z)), \end{aligned}$$

$$\frac{\gamma_n(z)}{\delta_n(z)} = \sqrt{\frac{2}{\pi z}} \left( \mp \mathrm{i} \right)^n \mathrm{e}^{\mp \mathrm{i}\pi/4} \left[ P_n'(z) - Q_n(z) \pm \mathrm{i} (Q_n'(z) + P_n(z)) - \frac{1}{2\pi} \left( P_n(z) \pm \mathrm{i} Q_n(z) \right) \right],$$

and  $P_n(z)$  and  $Q_n(z)$  are given in reference [47], we can show that the matrix  $\Pi(x, y)$  of equation (D19) reduces to

$$\Pi(x,y) = \begin{bmatrix}
\alpha_n(x) & 0 & \beta_n(x) & 0 \\
\gamma_n(x) & 0 & \delta_n(x) & 0 \\
0 & \alpha_n(y) & 0 & \beta_n(y) \\
0 & \gamma_n(y) & 0 & \delta_n(y)
\end{bmatrix} \mathbf{\Theta}(x,y) e^{in\varphi}$$
(D21)

where  $\Theta(x, y)$  is a 4 × 4 matrix function, with  $\theta_{11} = e^{ix}$ ,  $\theta_{23} = e^{iy}$ ,  $\theta_{32} = e^{-ix}$  and  $\theta_{44} = e^{-iy}$ ; all other elements are zero. Therefore, using equations (D15), (D17), (D18) and (D21), the state vectors may be written in forms similar to equation (5),

$$\mathbf{z}_{f} = \mathbf{E}_{f} \begin{bmatrix} \mathbf{u}_{f}^{o} \\ \mathbf{u}_{i}^{d} \end{bmatrix}, \qquad \mathbf{z}_{m} = \mathbf{E}_{m} \begin{bmatrix} \mathbf{u}_{m}^{o} \\ \mathbf{u}_{m}^{d} \end{bmatrix}, \tag{D22}$$

where

$$\begin{bmatrix} \mathbf{u}_{f}^{o} \\ \mathbf{u}_{f}^{i} \end{bmatrix} = \begin{bmatrix} A_{f}^{(1)} e^{\mathrm{i}cr} \\ B_{f}^{(1)} e^{-cr} \\ A_{f}^{(2)} e^{-\mathrm{i}cr} \\ B_{f}^{(2)} e^{\mathrm{c}r} \end{bmatrix}, \qquad \begin{bmatrix} \mathbf{u}_{m}^{o} \\ \mathbf{u}_{m}^{i} \end{bmatrix} = \begin{bmatrix} A_{m}^{(1)} e^{\mathrm{i}ar} \\ B_{m}^{(1)} e^{\mathrm{i}br} \\ A_{m}^{(2)} e^{-\mathrm{i}ar} \\ B_{m}^{(2)} e^{-\mathrm{i}br} \end{bmatrix},$$

$$\mathbf{r} = \mathbf{N}_{f}(r)\mathbf{\Theta}^{-1}(cr, \mathrm{i}cr), \qquad \mathbf{E}_{m}(r) = \mathbf{N}_{m}(r)\mathbf{\Theta}^{-1}(ar, br)$$

It can be shown that the wave vectors satisfy

$$\begin{bmatrix} \mathbf{u}_{f}^{o}(R) \\ \mathbf{u}_{f}^{i}(r) \end{bmatrix} = \operatorname{diag}\left(e^{\mathrm{i}c\tilde{d}}, e^{-c\tilde{d}}, e^{\mathrm{i}c\tilde{d}}, e^{-c\tilde{d}}\right) \begin{bmatrix} \mathbf{u}_{f}^{o}(r) \\ \mathbf{u}_{f}^{i}(R) \end{bmatrix}, \tag{D23}$$

$$\begin{bmatrix} \mathbf{u}_{m}^{o}(R) \\ \mathbf{u}_{m}^{i}(r) \end{bmatrix} = \operatorname{diag}(e^{\mathrm{i}a\tilde{d}}, e^{\mathrm{i}b\tilde{d}}, e^{\mathrm{i}a\tilde{d}}, e^{\mathrm{i}b\tilde{d}}) \begin{bmatrix} \mathbf{u}_{m}^{o}(r) \\ \mathbf{u}_{m}^{i}(R) \end{bmatrix}. \tag{D24}$$

These define the asymptotic S-matrices for the annular plates. Define

$$\Pi^{sld}(x, y) = 2 \begin{vmatrix}
J_n(x) & 0 & 0 & 0 \\
J'_n(x) & 0 & 0 & 0 \\
0 & 0 & J_n(y) & 0 \\
0 & 0 & J'_n(y) & 0
\end{vmatrix} e^{in\varphi},$$
(D25)

where  $J_n$ , are Bessel functions. It can then be shown that

$$\mathbf{z}_{\alpha}^{(f)} = \tilde{\mathbf{Y}}_{\alpha} \mathbf{z}_{\alpha}^{(v)}, \qquad \alpha = \text{ for } m,$$
 (D26)

where

$$\tilde{\mathbf{Y}}_{\alpha} = \begin{bmatrix} \frac{(N_{\alpha}^{sld})_{23}(N_{\alpha}^{sld})_{31} - (N_{\alpha}^{sld})_{21}(N_{\alpha}^{sld})_{33}}{-(N_{\alpha}^{sld})_{13}(N_{\alpha}^{sld})_{21} + (N_{\alpha}^{sld})_{11}(N_{\alpha}^{sld})_{33}} & \frac{(N_{\alpha}^{sld})_{13}(N_{\alpha}^{sld})_{31} - (N_{\alpha}^{sld})_{11}(N_{\alpha}^{sld})_{33}}{-(N_{\alpha}^{sld})_{13}(N_{\alpha}^{sld})_{21} - (N_{\alpha}^{sld})_{11}(N_{\alpha}^{sld})_{23}} & \frac{(N_{\alpha}^{sld})_{13}(N_{\alpha}^{sld})_{21} - (N_{\alpha}^{sld})_{11}(N_{\alpha}^{sld})_{23}}{-(N_{\alpha}^{sld})_{13}(N_{\alpha}^{sld})_{21} + (N_{\alpha}^{sld})_{11}(N_{\alpha}^{sld})_{23}} & \frac{(N_{\alpha}^{sld})_{13}(N_{\alpha}^{sld})_{41} - (N_{\alpha}^{sld})_{11}(N_{\alpha}^{sld})_{43}}{-(N_{\alpha}^{sld})_{13}(N_{\alpha}^{sld})_{21} + (N_{\alpha}^{sld})_{11}(N_{\alpha}^{sld})_{23}} & \frac{(N_{\alpha}^{sld})_{13}(N_{\alpha}^{sld})_{41} - (N_{\alpha}^{sld})_{11}(N_{\alpha}^{sld})_{43}}{(N_{\alpha}^{sld})_{13}(N_{\alpha}^{sld})_{21} - (N_{\alpha}^{sld})_{11}(N_{\alpha}^{sld})_{23}} & , \quad (D27)$$

and  $\mathbf{N}_{sd}^{sd} = \mathbf{N}_{e}\mathbf{\Pi}^{-1}(cr, icr)\mathbf{\Pi}^{sld}(cr, icr)$  and  $\mathbf{N}_{sd}^{sld} = \mathbf{N}_{ss}\mathbf{\Pi}^{-1}(ar, br)\mathbf{\Pi}^{sld}(ar, br)$ .

#### APPENDIX E: SCATTERING COEFFICIENTS OF A T-JUNCTION

The continuity conditions at a T-junction are, referring to Fig. 2,

$$\mathbf{Z}^{(f)}(X_2) = \mathbf{Z}^{(f)}(X_1) + \mathbf{z}^{(f)}(X_2), \qquad \mathbf{Z}^{(v)}(X_2) = \mathbf{Z}^{(v)}(X_1) = \mathbf{z}^{(v)}(X_2). \tag{E28}$$

These imply that the transmission and reflection coefficients are

$$\begin{split} \mathbf{R}_{(11)} &= -\mathbf{E}_2^{-1}(X_1)\mathbf{F}'[\mathbf{E}_3(X_1)\mathbf{E}_1(X_1)^{-1} + \mathbf{\tilde{E}}_3'(x_3)\mathbf{\tilde{E}}_1'(x_3)^{-1} - \mathbf{E}_3(X_2)\mathbf{E}_1(X_2)^{-1}]\mathbf{E}_1(X_1), \\ \mathbf{T}_{(12)} &= \mathbf{E}_2^{-1}(X_1)\mathbf{F}'[\mathbf{E}_4(X_2)\mathbf{E}_2(X_2)^{-1} - \mathbf{E}_3(X_2)\mathbf{E}_1(X_2)^{-1}]\mathbf{E}_2(X_2), \\ \mathbf{T}_{(13)} &= -\mathbf{E}_2^{-1}(X_1)\mathbf{F}'[\mathbf{\tilde{E}}_4'(x_3)\mathbf{\tilde{E}}_2'(x_3)^{-1} - \mathbf{\tilde{E}}_3'(x_3)\mathbf{\tilde{E}}_1'(x_3)^{-1}]\mathbf{\tilde{E}}_2'(x_3), \\ \mathbf{T}_{(21)} &= \mathbf{E}_1^{-1}(X_2)[\mathbf{E}_1(X_1) + \mathbf{E}_2(X_1)\mathbf{R}_{11}], \\ \mathbf{R}_{(22)} &= \mathbf{E}_1^{-1}(X_2)[\mathbf{E}_2(X_1)\mathbf{T}_{12} - \mathbf{E}_2(X_2)], \\ \mathbf{T}_{(23)} &= \mathbf{E}_1^{-1}(X_2)\mathbf{E}_2(X_1)\mathbf{T}_{13}, \\ \mathbf{T}_{(31)} &= \mathbf{\tilde{E}}_1'^{-1}(x_3)\mathbf{E}_1(X_2)\mathbf{T}_{21}, \\ \mathbf{T}_{(32)} &= \mathbf{\tilde{E}}_1'^{-1}(x_3)[\mathbf{E}_1(X_2)\mathbf{R}_{22} + \mathbf{E}_2(X_2)], \\ \mathbf{R}_{(33)} &= \mathbf{\tilde{E}}_1'^{-1}(x_3)[\mathbf{E}_1(X_2)\mathbf{T}_{23} - \mathbf{\tilde{E}}_2'(x_3)], \end{split}$$

where

$$\mathbf{F}' = [\mathbf{E}_4(X_1)\mathbf{E}_2(X_1)^{-1} + \tilde{\mathbf{E}}_3'(X_3)\tilde{\mathbf{E}}^{\prime}(X_3)^{-1} - \mathbf{E}_3(X_2)\mathbf{E}_1(X_2)^{-1}]^{-1}.$$